Arcata Fisheries Technical Report TR 2019-37

The Use Of Small 2-Dimensional Habitat Zones And Dual-Snorkeler Surveys To Model The Habitat Use Of Juvenile Salmonids In The Trinity River, California.

William D. Pinnix[1], Derek Rupert[1], Nicholas A. Som[1], Paul Petros[2], and Kyle De Juilio[3]

[1]U.S. Fish and Wildlife Service
Arcata Fish and Wildlife Office
1655 Heindon Road
Arcata, California 95521
(707) 822-7201

[2]Hoopa Valley Tribal Fisheries Department
Hoopa, California 95546
(530) 625-4267

[3]Yurok Tribal Fisheries Program
Weitchpec, California 95546
(530) 625-4130

August 2019

This study was conducted as part of the Trinity River Restoration Program, with financial support provided by the Bureau of Reclamation and the Arcata Fish and Wildlife Office, U.S. Fish and Wildlife Service.

The Arcata Fish and Wildlife Office Fisheries Program reports its study findings through two publication series. The **Arcata Fisheries Data Series** was established to provide timely dissemination of data to local managers and for inclusion in agency databases. The **Arcata Fisheries Technical Reports** publishes scientific findings from single and multi-year studies that have undergone more extensive peer review and statistical testing. Additionally, some study results are published in a variety of professional fisheries journals.

Key words: Juvenile Salmonid, Chinook Salmon, Coho Salmon, Habitat, 2-D Model, Trinity River

The correct citation for this report is:

Pinnix, W.D., D. Rupert, N.A. Som, P. Petros, and K. De Juilio 2019. The Use of Small 2-Dimensional Habitat Zones and Dual-Snorkeler Surveys to Model the Habitat Use of Juvenile Salmonids in the Trinity River, California. U.S. Fish and Wildlife Service. Arcata Fish and Wildlife Office, Arcata Fisheries Technical Report Number TR 2019-37, Arcata, California.

TABLE OF CONTENTS

LIST OF TABLES

LIST OF FIGURES

LIST OF APPENDICES

The Use Of Small 2-Dimensional Habitat Zones And Dual-Snorkeler Surveys To Model The Habitat Use Of Juvenile Salmonids In The Trinity River, California.

William D. Pinnix[1], Derek Rupert[1], Nicholas A. Som[1], Paul Petros[2], and Kyle De Juilio[3]

[1]U.S. Fish and Wildlife Service, Arcata Fish and Wildlife Office
1655 Heindon Road
Arcata, California 95521
bill_pinnix@fws.gov (corresponding author)

[2]Hoopa Valley Tribal Fisheries Department
P.O. Box 417
Hoopa, California 95546
ppetros@hoopa-nsn.gov

[3]Yurok Tribal Fisheries Program
Highway 96, Box 196, Weitchpec Route
Hoopa, California 95546
kdejuilio@yuroktribe.nsn.us

Executive Summary

In this report, we present a novel approach to assess the relationship between juvenile salmonid density and physical habitat characteristics on the upper Trinity River, California. This approach is based on an N-mixture statistical model that relies on many independent observations of juvenile salmonids in areas of homogenous habitat. We define homogeneous habitat as water that is +/- 0.15 m in depth and +/- 0.15 m/s in velocity. N-mixture models allow for simultaneous estimation of fish abundance and observor (snorkeler) error, but require a large number of observations given the number of parameters that are estimated. Homogenous polygons averaging 4.9 m^2 in area allowed 2 snorkelers to simultaneously count juvenile salmonids while ensuring closure (i.e., no fish entering or exiting the survey area during the survey). A total of 4,568 polygons were surveyed over a two-year period.

A variety of physical habitat characteristics were collected during the surveys to develop a descriptive model comparing the physical habitat attributes to juvenile salmonid density. These attributes included, but were not limited to, depth, velocity, adjacent velocity, distance to cover, cover type, and distance to bank. Juvenile salmonid density is presented in reference to these attributes to aid in comparisons to past studies and for visual reference. The results from the N-mixture model suggest that although

simple measures of juvenile salmon habitat (depth, velocity, distance to cover) do influence juvenile salmon abundance (and hence density), ideal conditions exist (as suggested by the importance of the quadratic terms), and the interaction of such habitat conditions has a significant effect. Of the three basic characteristics, depth was the least informative in the overall model, but is an important interaction term with velocity and distance to cover.

Posterior distribution estimates indicated that detection probability decreased with increasing depths and among snorkelers, with average snorkeler detection rate estimates ranging from 0.76 to 0.92. The probability of a site containing any juvenile Chinook Salmon at all decreased with increasing water depth, velocity, and distance to cover; given juvenile Chinook Salmon were present, the posterior distributions suggested that abundance decreased with increasing distance from escape cover. Nearly all habitat metrics collected for each polygon appear to provide important insights into the range of density at which juvenile salmonids occupy habitats in the Trinity River. Strongest of these appears to be water velocity. The relationship between density of juvenile Chinook Salmon and distance to cover was an important parameter in zero-inflation and abundance portions of the statistical model.

The integrated habitat assessment plan (IHAP), that uses habitat guilds to describe where fish are most abundant, was supported by the robust dataset collected during this study. Our finding here generally supports the IHAP habitat guilds, especially the zero-inflation portion of the model that predicts presence or absence of juvenile salmonids based on depth, velocity and distance to cover. However, the abundance portion of the model also included quadratic and interaction terms that show a more complex picture of the distribution of juvenile Chinook Salmon than can be predicted from IHAP habitat guilds.

This project was initiated with the goal of estimating the association of fish abundance (or density) with physical habitat characteristics to inform the SSS Chinook Salmon population dynamics model. Habitat availability is often expressed in population dynamics models via a habitat suitability index (HSI). HSI values range between 0 (lower bound representing least unsuitable habitat) and 1 (upper bound representing the most suitable habitats). The probability distribution (zero-inflated Poisson) employed in our statistical modeling makes HSI implementation very straightforward. By incorporating the posterior variation for each parameter, the generated HSI values can even reflect the parameter uncertainty of our model.

INTRODUCTION

The Trinity River's populations of native, anadromous fish have been reduced because of various anthropogenic activities, including mining, timber harvest, dam construction, and water diversion. Such practices have led to truncated and degraded freshwater habitats for Chinook salmon (*Oncorhynchus tshawytscha*), Coho Salmon (*O.kisutch*), and steelhead trout (*O. mykiss*) in the Trinity River (USFWS and HVT 1999). Despite a hatchery mitigation program, a precipitous collapse of naturally-produced salmonid stocks followed the development and operation of the Trinity River Division (TRD) of the Central Valley Project (CVP) in the 1960s, which resulted in the construction of Trinity and Lewiston Dams and subsequent water diversions.

Trinity River fish stocks hold cultural, economic, and social significance to native peoples, residents, and commercial and sport fisheries. Since the early 1970s, many groups have attempted to recover the anadromous fish runs of the Trinity River. The Trinity River Restoration Program (TRRP) was established in 2000 to restore the fishery resources of the Trinity River that were adversely affected by construction and operation of the TRD (USDOI 2000). Restoration actions have included mechanical channel rehabilitation, flow management, coarse sediment augmentation, and watershed restoration. These activities are to be conducted as part of an adaptive management program so that outcomes of management actions can be evaluated and improved. In 2014, the restoration activities implemented by the TRRP were independently evaluated by the TRRP Science Advisory Board (SAB) and summarized in the *Review of the Trinity River Restoration Program's Channel Rehabilitation Strategy, Phase 1* (Phase 1 Review; Buffington et al. 2014).

In the Phase 1 Review, the SAB highlighted the need for and utility of a fish production model due to the slow physical and biological response times involved in restoration. Fish production modeling can be used to test hypotheses about relative effects that various restoration and management activities may have on fish populations. In 2014, the TRRP initiated the development of a juvenile Chinook salmon production model, known as the stream salmonid simulator (SSS; Polos 2013). Many of the TRRP's monitoring programs, such as hydraulic modeling (Alvarez et al. 2015), juvenile fish habitat assessments (Goodman et al. 2010, De Juilio et al. 2014), juvenile salmonid emigration monitoring (Petros et al. 2015, Harris et al. 2016), and adult salmon redd and carcass surveys (Chamberlain et al. 2012), supplied crucial data for development of multiple sub-models to support the SSS fish production model.

The TRRP Integrated Assessment Plan (IAP) version 1.0 (TRRP and ESSA 2009) states: "changes in the abundance or density of juveniles over time and in relation to parental spawner abundance produced from the upper Trinity River is the primary metric proposed for assessing whether rehabilitation and flow actions have increased natural salmonid production." One of the key performance measures in section 3.2.1 of the IAP is fry density and abundance. A data gap identified by the TRRP fish workgroup is the link between juvenile Chinook salmon density and specific physical habitat measures. Although the fish density study (Pinnix et al. 2016) found a relationship between juvenile salmonid density and physical habitat, the scale of the habitat measurements was too coarse to inform a fish production model. Finer scale data were needed to create an equation linking the biological response to the physical environment (i.e., fish density as a function of physical covariates) to aid in development, calibration, and validation of the fish production model (Polos 2013).

The goal of this project is to assess the density of juvenile Chinook salmon in the restoration reach of the mainstem Trinity River (Lewiston Dam to confluence with North Fork Trinity River) over a range of hydraulic and cover conditions during the primary rearing period. In addition, sampling was co-located at sites where the TRRP has developed two-dimensional (2-D) hydraulic models to aid in the linking of the biological response to changes in physical habitat parameters. This report presents the methodology used in collecting fish density data and includes summary statistics associated with the collected data. A companion manuscript will present the statistical modeling associated with the data described herein, and the resulting equations for assigning habitat quantities in the restoration reach as it relates to the SSS model.

METHODS

Study Area

The Trinity River is in northwestern California (Figure 1). The headwaters are in the Trinity Mountains, from which it flows 274 river km (RKM) to its confluence with the Klamath River. The watershed has a drainage area of 7,679 km^2, approximately one quarter of which is upstream of Lewiston Dam, the upstream limit of anadromous fish passage (USFWS 1989, USBOR 2009). The TRRP restoration reach is defined as the 64 RKM of mainstem Trinity River below Lewiston Dam to the confluence with the North Fork Trinity River.

Nine of the eleven 400-m 2-D hydraulic models developed in 2010 (Alvarez et al. 2015) to support assessment of streamflow to habitat relationships (Goodman et al. 2010) were utilized for this study (Figure 1). Two sites were unusable at the time of this study due to the morphology of one site being altered via channel rehabilitation and the model for the other site not meeting calibration and validation standards. Sites were given names that reflect their location on the river, arranged here in order of increasing distance from Lewiston dam (DFD; see Figure 1 and Table 1); Cableway (DFD 2.6km), Bucktail (DFD 9.3km), McIntyre (DFD 23.0km), Indian Creek Boat Access (DFD 26.5km), Indian Creek Side Channel (DFD 28.5km), Evan's Bar (DFD 44.6km), Round House (DFD 46.2km), Sheridan (DFD 48.1km), and Valdor (DFD 59.4km).

Table 1. Descriptions of the nine 400m study locations.

	Distance from Lewiston Dam (km)	2D Model Approximate to Winter Base Flow (cfs)	Surface Area at Winter Base Flow (m^2)	Surface Area with Cover (m^2) [% of total]	Bank Length (m)	Side Channel?	TRRP Rehab Site	USGS Gauge
Cableway	2.6	300	13,180	1619 [12.3%]	1824	Yes, large	Yes, 2008	1152550
Bucktail	9.3	300	10,442	977 [9.4%]	1218	Yes, small	Yes, 2008	1152550 + 11525530
McIntyre	23.0	300	12,769	1548 [12.1%]	1580	Yes, small	No	11525655
Indian Cr Boat Access	26.6	300	11,257	2069 [18.4%]	1633	No, split channel	No	11525655 + 11525670
Indian Cr Side Channel	28.5	450	13,081	2278 [17.4%]	1851	Yes, large	Yes, 2007	11525655 + 11525670
Evans Bar	44.6	550	14,201	1594 [11.2%]	897	No	No	11526250
Roundhouse	46.2	550	11,048	1365 [12.4%]	1034	No	No	11526250
Sheridan	48.1	700	15,038	1299 [8.6%]	951	No	No	11526250
Valdor	59.4	777	15,504	763 [4.9%]	943	No	Yes, 2006	11526400

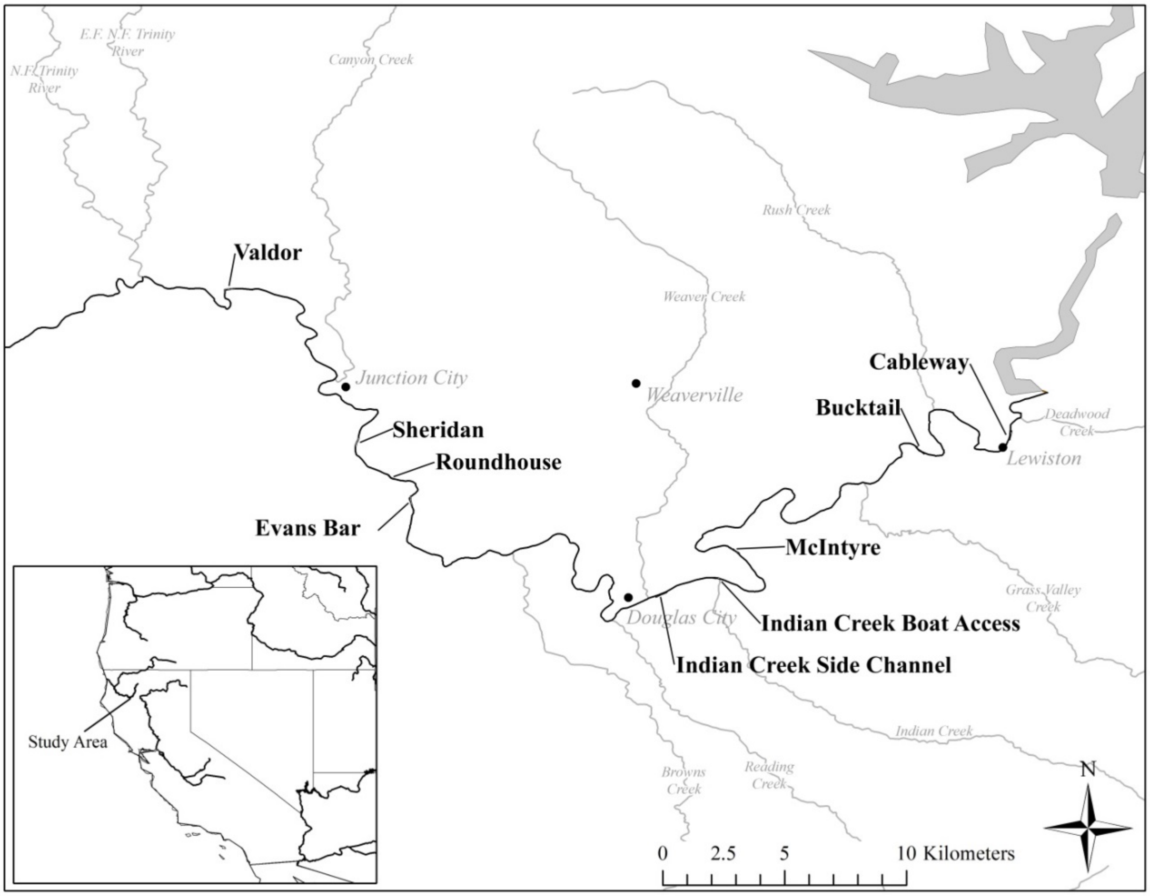

Figure 1. Survey locations on the Trinity River arranged in order of their distance from Lewiston Dam (DFD); Cableway (2.6 km DFD), Bucktail (9.3 km DFD), McIntyre (23 km DFD), Indian Creek Boat Access (26.5 km DFD), Indian Creek Side Channel (28.5 km DFD), Evan's Bar (44.6 km DFD), Round House (46.2 km DFD), Sheridan (48.1 km DFD), and Valdor (59.4 km DFD).

Statistical Approach

Data collected for this project allowed the simultaneous estimation of fish density relationships with physical habitat characteristics and the detection efficiency of snorkelers. To accomplish this, the data collection and subsequent statistical analyses followed a framework commonly referred to as N-mixture modeling. These models were first attributed to Royle (2004), who showed that by conducting independent replicate surveys, one could estimate detection efficiency and hence the true local abundance (N) at each sampling location. Although the N values might be of interest in many cases, these models are also used to test the effects of covariates to explain variation in the distribution of organisms (Graves et al. 2011), while accounting for imperfect detection to avoid biases in estimates (Kery 2008).

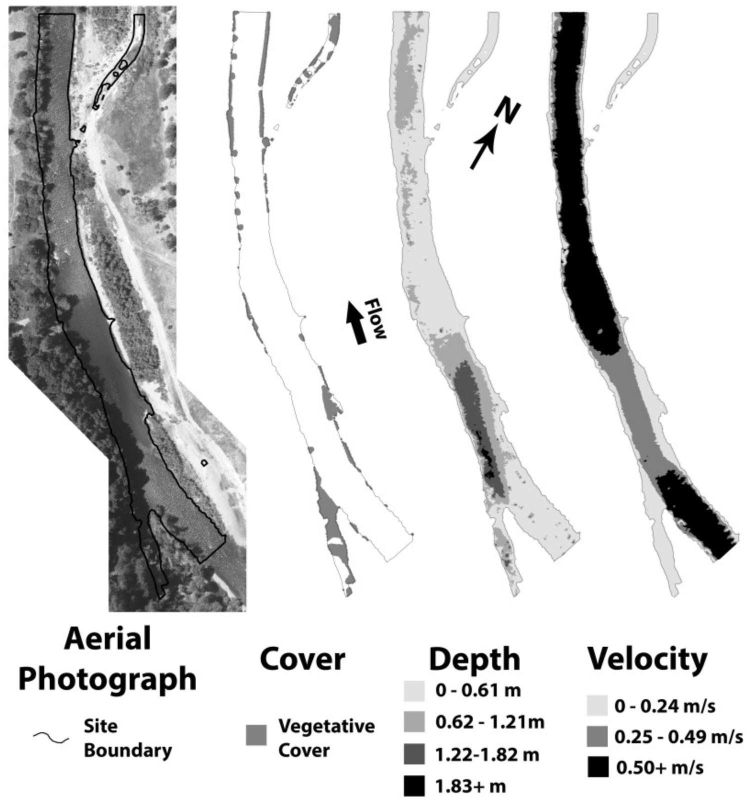

Figure 2. Visual representation of the 2-D hydraulic model at Bucktail ($8.5 m^3 s^{-1}$). Although a continuum of depth and velocities are present in the model, here they are shown categorically to match the habitat type bins used to select sample sites.

2-D Models

Outputs from 2-D hydraulic models were used to distribute sampling effort throughout a wide range of depth, velocity, and cover combinations at each sampling site. Each 2-D hydraulic model provided a map of existing cover and, given a discharge value, predicted depth and velocity at contiguous 1-m^2 nodes across the site. When displayed visually, these site-specific models predicted where physical variable combinations occurred at a given discharge (Figure 2 and Figure 3). Model output for several river discharges (~$4.25 m^3 s^{-1}$ increments), from 8.5 $m^3 s^{-1}$ (300 cfs) to 56.6 $m^3 s^{-1}$ (2000 cfs), were generated for each site. Prior to a sampling event, the model output closest in discharge was selected based on the anticipated discharge at a site during surveys to aid in sample selection, as described below. Tributary accretion resulted in higher winter base flows at sites further downstream from Lewiston Dam, such that different sites used output from different discharge levels.

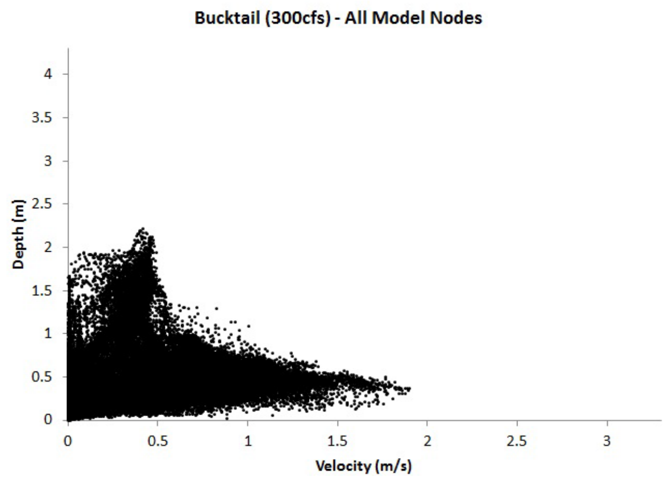

Figure 3. Example of distribution of model nodes (Bucktail site) at approximate winter base flow ($8.5m^3s^{-1}$).

Sampling Design

Regression model-based sampling design principles were utilized to allocate samples over various depth, velocity, and distance to cover combinations (Kiefer 1958). To efficiently detect relationships that might be non-linear, or to estimate interacting effects among the suite of explanatory variables, samples were collected across the mutually occurring combinations of the explanatory variables with the greatest contrast.

For each sampling occasion at each 2-D site, between 60 and 75 sampling locations were selected by first weighting the sampling locations according to the optimality principles described above, and then stratifying replicate surveys spatially along the length of the 2-D site, as described below. First, the 2-D model predictions of depth and velocity at each 1-m^2 node were obtained. The bivariate depth and velocity distribution at a 2-D site were plotted and overlaid with a grid representing bins of differing combinations of depth and velocity (Figure 4, Table 2). To evaluate the effects of depth and velocity, as well as the potential for interactions and non-linear effects, most sampling effort was allocated to the most extreme bins, with a smaller number of samples from intermediate bins (Figure 4). To select the exact 2-D node locations of sampling within each bin, the possible locations were sorted by their distance from Lewiston Dam, and the nodes were selected via spatial stratification to capture sampling locations along the entire 2-D site and spatially balance the samples. The process was repeated separately for all nodes within 1 m of fish escape cover and those not near cover, this allowed the further exploration of interactions of depth and velocity with distance from cover (Figure 4). A new set of sampling locations was generated, according to the methods described above, for each 2-D site visit (Figure 5).

To address the closure assumption required by the N-mixture models, replicate surveys via paired snorkeler counts were conducted, where two snorkelers simultaneously and independently surveyed the selected area and reported their number of counted juvenile salmonids.

Table 2. Map codes used to specify the habitat type bins used to distribute sampling effort throughout a site.

Code	Cover	Velocity (m/s)		Depth (m)	
A	Yes	High	>0.50	Low	<0.61
B	Yes	High	>0.50	Moderate	0.62-1.21
C	Yes	Low	<0.25	High	1.22-1.83
D	Yes	Low	<0.25	Low	<0.61
E	Yes	Low	<0.25	Moderate	0.62-1.21
F	Yes	Moderate	0.26-0.49	High	1.22-1.83
G	Yes	Moderate	0.26-0.49	Low	<0.61
H	Yes	Moderate	0.26-0.49	Moderate	0.62-1.21
I	No	High	>0.50	Low	<0.61
J	No	High	>0.50	Moderate	0.62-1.21
K	No	Low	<0.25	High	1.22-1.83
L	No	Low	<0.25	Low	<0.61
M	No	Low	<0.25	Moderate	0.62-1.21
N	No	Moderate	0.26-0.49	High	1.22-1.83
O	No	Moderate	0.26-0.49	Low	<0.61
P	No	Moderate	0.26-0.49	Moderate	0.62-1.21

Because extremely fast and deep water is difficult to snorkel in an upstream direction, all nodes >1.83m in depth and those that were both >1.22m in depth and >0.50m/s in velocity were removed from consideration and not snorkeled. Not all habitat categories exist in all the model outputs (e.g., there were not any cover nodes, 0.62-1.21m in depth and >0.50m/s in velocity for the Bucktail site at 8.5m^3s^{-1}).

Equipment

This project relied heavily on global positioning system (GPS) equipment and capabilities to accurately record geo-referenced locations. Specifically, Mobile Demand T-8700 tablet computers, Trimble ProXH GPS™ with Zephyr™ geodetic antenna, and Laser Technologies Trupulse™ 360 and 360B laser rangefinders were used to record and offset geo-referenced locations. This hardware, when paired with Trimble TerraSync™ survey software, allowed real-time GPS mapping in the field. These capabilities permitted field crews to locate pre-specified points, mark polygon vertices, draw polygon perimeters, and record physical and biological data. All GPS data was collected and projected in the coordinate system NAD1983 State Plane California I FIPS 0401 (US survey feet). The horizontal accuracy was assumed to be +/- 0.2m from GPS positions and +/- 0.3m from positions offset with laser rangefinders. Water velocities and depths were measured with SonTek Flowtracker™ acoustic doppler velocimeters paired with Rickly Hydrological Company top-setting wading rods.

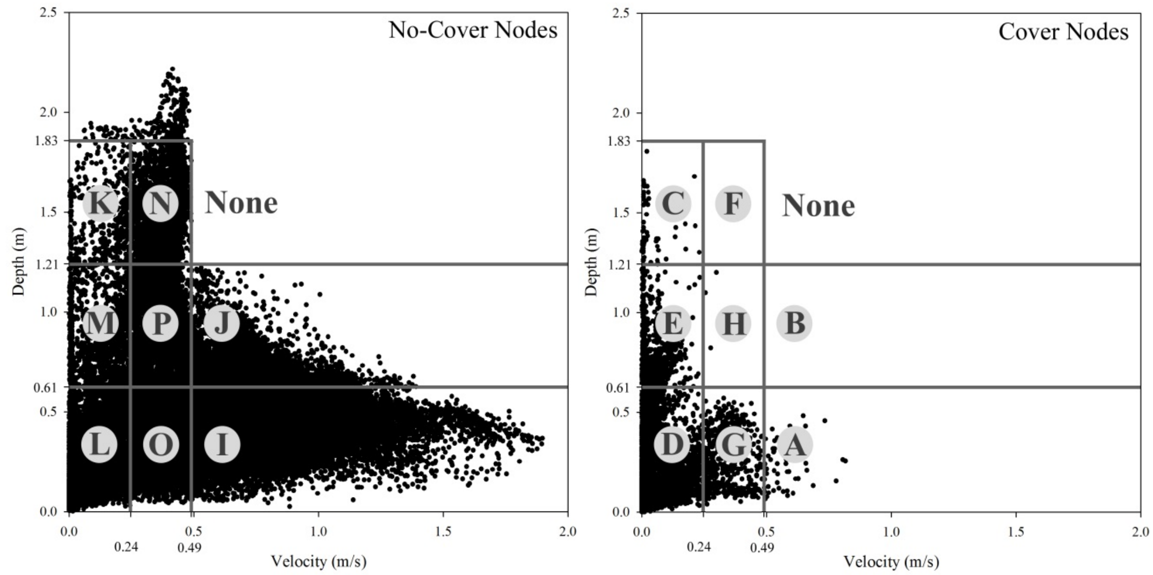

Figure 4. Plot of the 16 habitat-type bins with codes, showing the model nodes from the Bucktail site at $8.5 m^3 s^{-1}$. Notice that the cover nodes are few or not present in some of the bin types. See Table 2 for the values used for each habitat type-code.

Survey Implementation

Surveying was carried out in 2013-2014 and was completed in two phases: (1) site set-up and (2) snorkel survey counts. Two 3-5 person crews worked in an upstream direction through the sites during the polygon set-up and snorkel surveys. Crews were assigned either river-left or river-right banks. Where side channels were present, crews were divided between the main channel and the side channel. An attempt was made to survey all nine sites within a two-week period. Each two-week period constituted one “round” of sampling. Rounds were labeled 1 through 9, with round 1 beginning in calendar week 7 (second week in February). Round 1 was not surveyed in 2013, but it is a place holder to maintain a consistent time frame between years. The order in which the sites were visited during a sampling round was managed around changing environmental conditions such as river discharge.

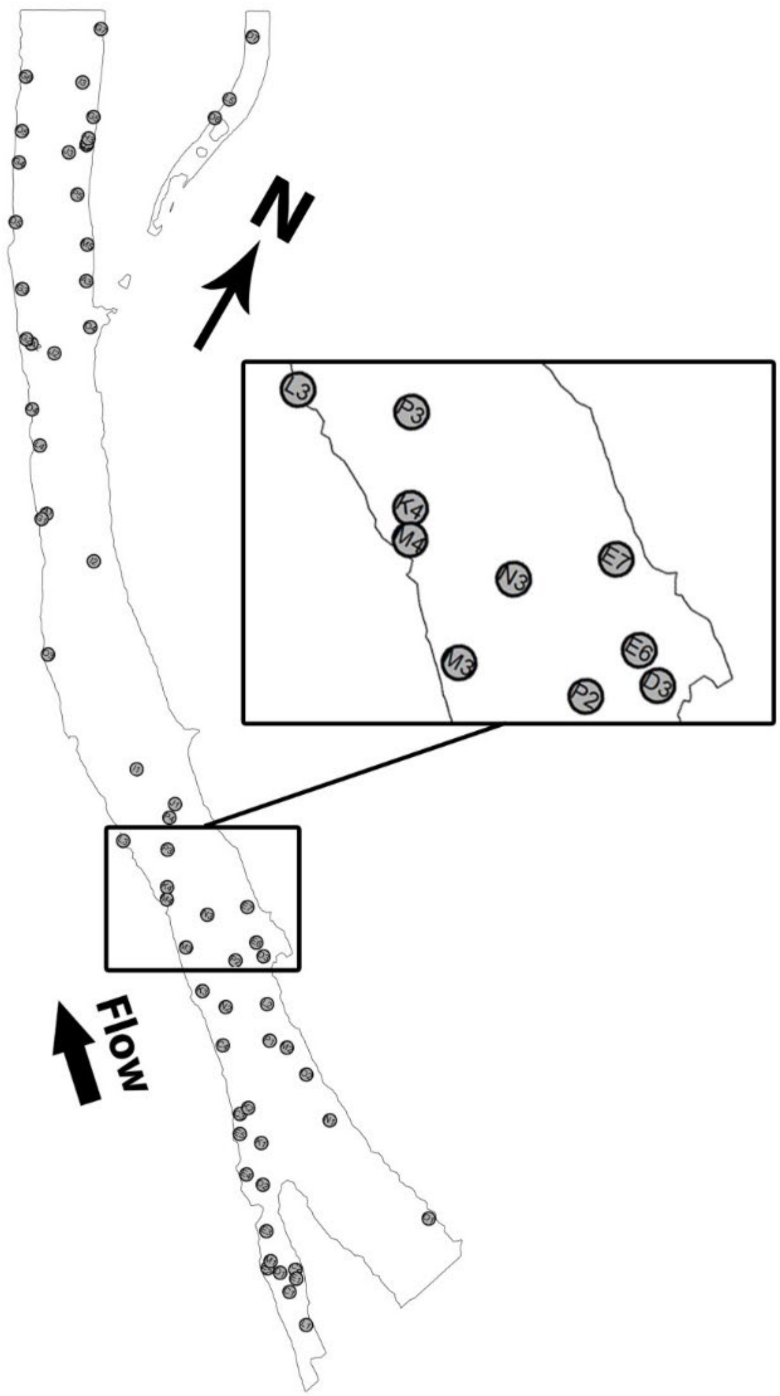

Figure 5. Example sampling map of the Bucktail site. Each of the 65 dots is coded, specifying the habitat type expected to exist at that location. This map informs the field crew what type of polygon to build and where to build it. Area enlarged to show detail.

Figure 6. Painted steel washers marked the start (green [lower three stacks], downstream) and end (orange [upper three stacks], upstream) of the polygons.

Site set-up: During the set-up phase, crews used GPS equipment to locate pre-selected individual sample points in the river channel. Once a sample point was located, the crew would evaluate the area and attempt to locate the habitat type specified by that point. If the specified habitat type could not be located at the pre-selected point, the crew would locate and construct a polygon at the nearest specified habitat type within 30 m. If the specified habitat could not be located within 30 m of the pre-selected point, the habitat criteria for either depth or velocity would be adjusted to match available depth/velocity/cover features. If the specified habitat type could not be found within 30 m of the point and the available habitat around that point was significantly different from the specified habitat bin, the crew would skip that point. Many more points were pre-selected than intended to survey, which allowed points to be skipped while still retaining the desired variation in habitat and sample size.

Once the habitat type was located, the crew would create a polygon delineating a zone of homogenous habitat. In this study, a polygon was a 2-D area of similar habitat (homogenous) in terms of water velocity, water depth, and cover. Homogeneity was defined as variation in water depth and velocity within the polygon that did not exceed +/- 0.15 m and +/- 0.15 m/s, respectively. Exceptions to these limits were made for polygons with cover and/or a bank edge because these polygons contain, if only marginally, areas of zero depth and velocity. The entirety of no-cover polygons were at least 1 m from any cover, while no part of a cover polygon was more than 1 m from cover.

The corners of each polygon were marked with either painted rocks or painted 3-inch steel washers (Figure 6). To aid the snorkelers in differentiating between closely spaced polygons, fluorescent-green makers were used on the downstream corners (start) and fluorescent-orange on the upstream corners (end). The size and shape of the polygon varied with amount of available homogenous habitat. In general, polygons were rectangular, and did not overlap or share edges. Crews were instructed not to build polygons in less than 0.06 m of water (too shallow to snorkel) or more than 1.83 m deep (too deep to snorkel), and the polygons were not to exceed 2 m in width (visibility range of species identification by snorkelers).

Once a polygon was established, the corners were marked with GPS equipment through the Terrasync software. Digital lines were drawn to connect the corners, forming a digital polygon. Each digital polygon was then attributed with numerous physical and habitat characteristics. Quality control procedures were carried out continuously as the data was being collected and entered, reducing measurement and recording errors. Below are descriptions of measured habitat characteristics and how they were obtained (See Appendix A for an example data table).

Water Depth of Polygon – Water depth was measured at a point within the polygon that the crew agreed best represented the polygon's depth. Depths were measured to the nearest 0.3048 m (1 ft). Polygons with a depth of 1.22-1.83 m were estimated by the crew, as the wading rods used were 1.22 m tall.

Water Velocity of Polygon – Water velocity was measured at a point within the polygon that the crew agreed best represented the polygon's water velocity. Velocities were measured at 60% of the water column depth to the nearest 0.003048 m/s (0.01 ft/s). On the rare occasions that negative velocities were measured, they were treated as positive. Polygon velocities were estimated or measured at approximately 60% water column depth if the depth exceeded the wading rods height of 1.22 m.

Adjacent Depth and Velocity – A secondary water depth and velocity was recorded from a point adjacent to the polygon. These measurements were taken on the thalweg side of the polygon in an area that best represented water velocity and depth flowing past the edge of the polygon.

Mainstem and Off Channel – Any polygons that were found outside the main channel (i.e. inside a side channel or alcove) were designated as off-channel. Off-channel polygons were identified at the following sites; Cableway, Bucktail, McIntyre, and Indian Creek Side Channel.

Substrate – The dominant surface substrate within each polygon was attributed to one of six categories; silt (>1 mm), sand (1-4 mm), gravel (5-75 mm), cobble (75-500 mm), boulder (>500 mm), or bedrock. The crew would confer over which category best represented the substrate of the polygon. The substrate category was recorded only during the 2014 sampling season.

Cover Type – The cover type associated with each polygon was recorded as one of nine categories; none, small woody debris (diameter < 100 mm), large woody debris (diameter > 100 mm), live trees, live willows (*Salix spp.*), grasses, aquatic vegetation (vascular plants), blackberry (*Rubus spp.*), or undercut bank. Algal periphyton was not treated as cover.

Distance to Cover – If a polygon had cover, it was designated as 0 m to cover. If the polygon was outside of cover, the distance from the polygon centroid was measured to the nearest cover. All no-cover polygons were built at least 1 m from cover. Distance to cover was measured with a laser range finder or estimated by the crew. Cover type was also recorded.

Cover Density – If cover was present, the volume of cover density was recorded as one of four percentile categories; 1-25% (very sparse cover), 26-50%, 51-75%, and 76-100% (very dense cover). The cover density category was recorded only during the 2014 sampling season.

Distance to Bank – If a polygon shared an edge with the bank, it was designated as a bank polygon (2013 data only). During the 2014 season, the distance from the bank to the polygon centroid was measured using a laser rangefinder or were estimated by the crew.

Snorkel survey: The second phase of a site visit was the snorkel surveys, completed after a polygon reset period of at least 24 hours. This allowed fish to redistribute to a natural state after the disruption during the polygon set-up process. Snorkel surveys were always completed mid-day (11:00 – 16:00 PST) to maintain consistency and reduce variability caused by possible diurnal changes in fish behavior.

Snorkel surveys were performed by two snorkelers, who enumerated juvenile salmonids (fish) within each polygon. The snorkelers simultaneously worked upstream in parallel counting fish within the boundaries of each polygon (Figure 7). To maintain consistency, a pair of snorkelers snorkeled together for an entire day; and these partners worked together across the season as much as possible. Snorkelers counted juvenile fish of each salmonid species (Chinook Salmon, Coho Salmon, steelhead trout, and brown trout) within two size classes (fry: 0-50mm; and presmolt: >50mm), however, all analyses relied on a sum of the two size categories within each species. Juvenile fish are defined as any salmonid that is not an adult (i.e., fish that are 1+ year old were counted as juveniles with the age-0 fish born that year). There were no attempts to distinguish between hatchery-produced and natural-origin juvenile salmonids, as it is not possible to do so in the field. Snorkelers counted only those fish that were seen holding within polygon boundaries prior to the onset of enumeration; those that entered the polygon subsequently were ignored. Snorkelers surreptitiously communicated their fish counts to data collectors to maintain independence between the counts. Data collectors attributed each polygon with the snorkeler names, snorkel location (i.e. bank-side or thalweg-side), observed water visibility, and fish counts, noting any unintended disturbances or unique situations.

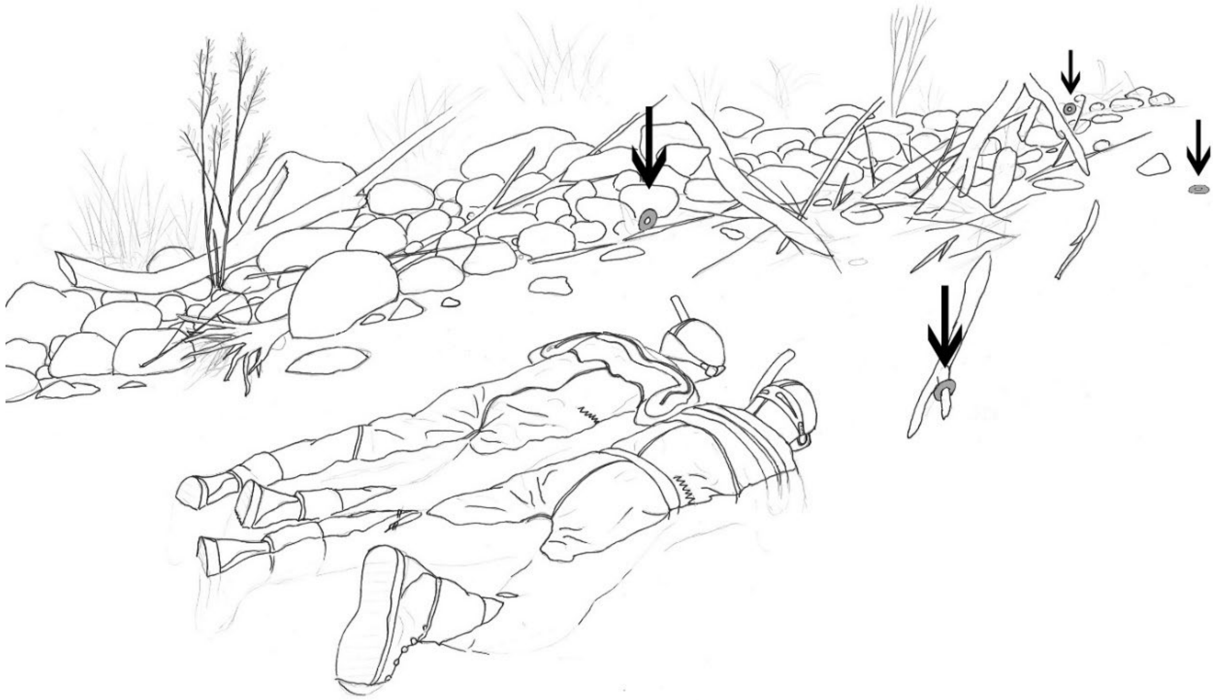

Figure 7. Snorkelers moved in parallel upstream with each snorkeler keeping a separate count of the fish in the polygons. Notice the gray circles upstream of the snorkelers representing the corners of a polygon.

Data Management

At the end of each round of data collection, all Terrasync files were processed through Trimble Pathfinder Office and exported as an ESRI shapefile. Each of these data files was reviewed and quality checked to ensure that data were recorded accurately and completely. Any polygon with data noted as unreliable (e.g., disturbed fish) was removed from the data set.

At the end of the season of data collection, all individual data files were merged. The area of each polygon was calculated with the *calculate area* tool in ArcMap (v. 10.1). Additional fields were added, including estimated river discharge and water temperature obtained from nearby USGS gages. Data originally recorded in standard units were converted to metric units.

Data Summaries

Fish Density: This report applies an observation-based density-per-species calculation to display and summarize data collected over the two years of sampling to evaluate how density relates to univariate habitat variables. This preliminary data summary provides insight into which variables appear to explain most of the variation, which then informs the second phase of data analysis as previously described. This data summary does not evaluate interdependence, co-variation, or detectability, nor has the overall statistical rigor of the N-mixture model been determined. For this data summary, the density (fish/m^2) of each species was calculated using the following equation:

$$d_{s,i} = \frac{Max[C_{s,i,j}, C_{s,i,j}]}{A_i}$$

Where: d = species density, s = species-size combination, i = polygon, C = snorkeler count, j = snorkeler, and A = area.

The maximum of the two snorkeler's counts was used to calculate fish density rather than the average of the two snorkeler's counts, because past snorkel survey studies have reported fish detection rates below 100% (Hillman et al. 1992). That is, it is more likely that snorkelers under-detect rather than over-detect fish counts.

Box and whisker plots are presented displaying fish density by species, sampling round, and distance from dam (site) to illustrate apparent relationships of fish density and measured habitat characteristics and allow readers to visualize the full range and variability of fish density observed within binned categories.

Statistical Model Selection and Fitting: The statistical model described in this report was only applied to juvenile Chinook Salmon, as that is the primary species of interest for the TRRP. As noted above, the sampling design and associated analysis of these data follow from the N-mixture modeling framework, where the observed data arise from the mixture of a process governing the true local abundances (N) at each location and a separate process governing the observation error. As the data collection for this project was initiated when salmonid fry emergence was relatively low and because the restoration reach represents a potentially under-seeded system, we assumed that our data might contain many observations where zero juveniles were observed; too many zeroes, perhaps, to conform to the behavior of standard statistical count distributions. Hence, we opted to model the process generating the true local abundances according to a zero-inflated Poisson distribution, which allows covariates to be associated with not only the size of counts at individual locations, but additionally, the preponderance of zeroes. In our model this count process is mixed with a binomial distribution describing the probability of detection at each sampling location. We also note a key component of these models is the ability to include the sample location area so that inference based on the effects of covariates can be expressed with respect to fish density.

A companion manuscript (Som et al. 2017) describes the Bayesian hierarchical statistical model used to estimate the effects of depth, velocity, and distance to cover over space and time on the local abundances of juvenile fish, and the effects of snorkeler variability, physical conditions, space, and time on the probability of detection at the sampling locations. For the abundance component of this model, interactions among the physical covariates are explored, as well as the potential for non-linear quadratic effects.

RESULTS

Weather and Water Years

In 2013 and 2014, the Trinity River received less than average precipitation during the sampling periods; 2013 was a dry water year (TRRP 2014) and 2014 was a critically dry water year (TRRP 2015). Precipitation events in 2013 had little effect on river discharge (Figure 8). In 2014, moderate rain events caused spikes in discharge, but the river quickly returned to low discharge conditions (Figure 9). The TRRP implements spring high flow releases (ROD flows) from Lewiston Dam. In 2013 and 2014, these flow releases began around April 20th (Figure 8 and Figure 9). In 2013, the flow event peaked with Lewiston Dam releasing 127.4 m^3s^{-1} (4,500 cfs), while in 2014 a peak of only 42.4 m^3s^{-1} was reached. One round of sampling in 2013 occurred on a stable bench of 56.6 m^3s^{-1} during the ascending limb of the hydrograph. In 2014, three rounds were conducted during the ROD flows, one during the extended peak of 42.4 m^3s^{-1} and two rounds during the descending limb over a range of flow conditions from 12.7 m^3s^{-1} to 34.0 m^3s^{-1}.

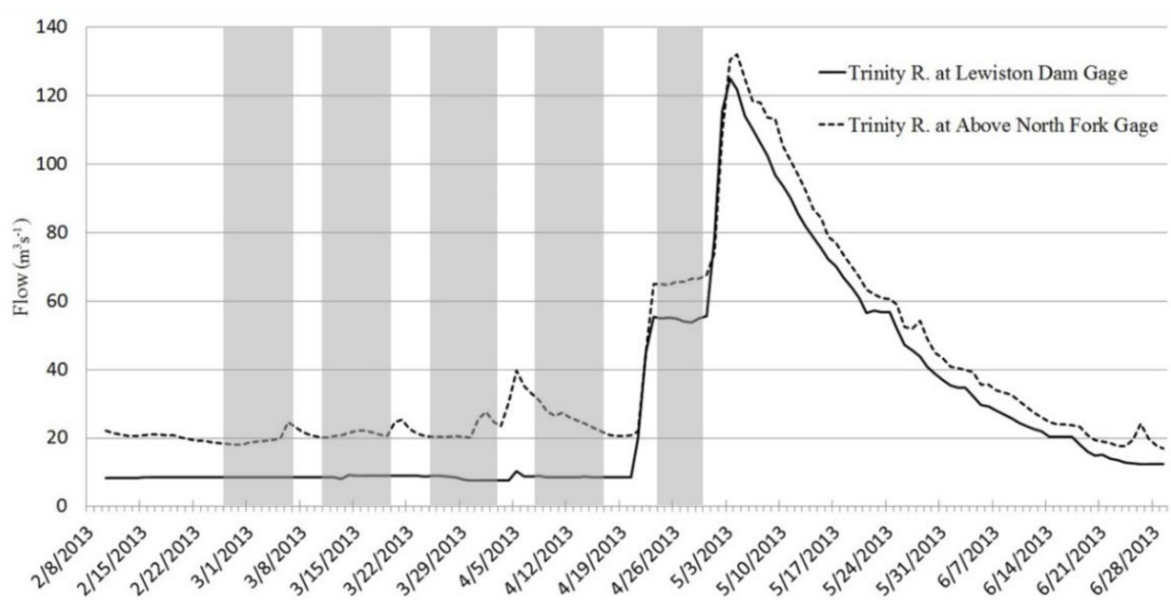

Figure 8. Discharge of water from Lewiston Dam (USGS gage 11525500) and flow of the Trinity River above the North Fork confluence (USGS gage 11526400) in 2013. The grey vertical bars represent the sampling periods (each an individual sampling round).

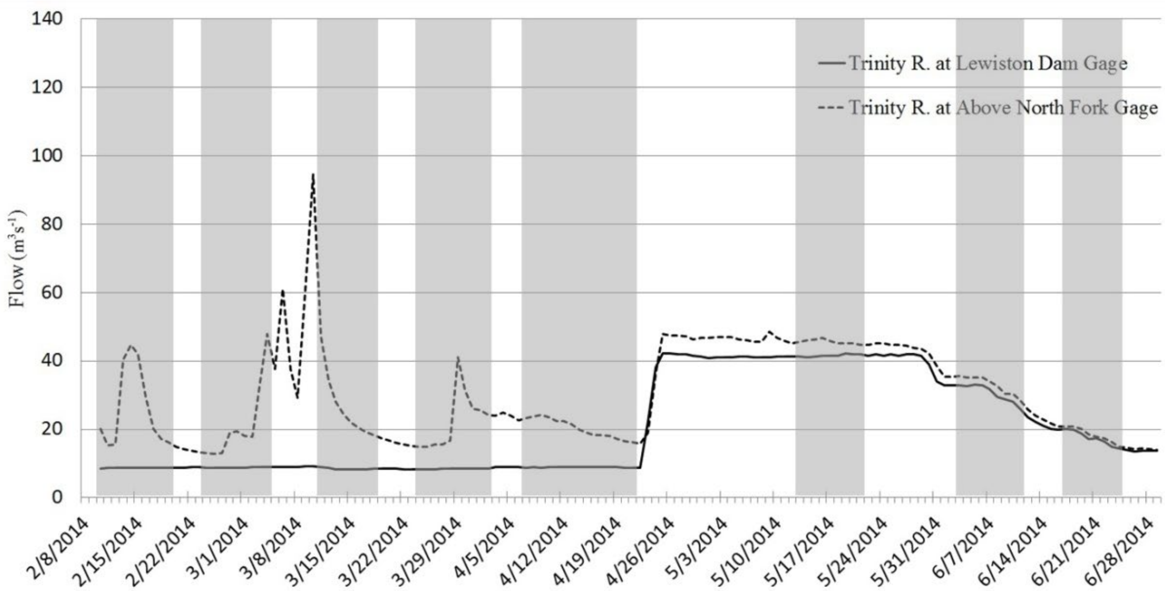

Figure 9. Discharge of water from Lewiston Dam (USGS gage 11525500) and flow of the Trinity River above the North Fork confluence (USGS gage 11526400) in 2014. The grey vertical bars represent the sampling periods (each an individual sampling round).

Polygons

In 2013, five rounds (rounds 2-6) of sampling were completed from February 26 to April 30, with 1,825 polygons created (Appendix A). In 2014, eight rounds (rounds 1-5, 7-9) of sampling were completed from February 10 to June 25, creating 2,743 polygons (Appendix B). The size of polygons ranged from 0.3 m^2 to 42.5 m^2, with a median of 3.8 m^2 and mean of 4.6 m^2. Sample collection was extended in 2014 to investigate changes that may occur in juvenile density after the release of ~2,000,000 hatchery juvenile Chinook Salmon.

Because sampling time frames each year did not cover the same number of weeks, year-to-year comparisons used rounds 2-5 which occurred during both years of sampling. Due to ROD spring hydrographs, low visibility and fluctuations in discharge sampling did not occur during round 7 of 2013 and round 6 of 2014. Because round 6 in 2013 and round 7 in 2014 were conducted at a similar discharge and time of year relative to ROD flows, they were used in the year-to-year comparisons.

Sample Distribution

The sample selection method distributed polygons spatially throughout each site (Figure 10) and across a wide range of depths and velocities (Figure 11). This sampling design also distributed sampling throughout a wide range of distance to cover measurements, distance to bank measurements, cover density values, and adjacent velocities. However, this sampling design did not appear to distribute sampling evenly across all types of cover, as some cover types (e.g. horsetails, live trees, and grasses) were available to fish only during high flows which were uncommon during our survey period.

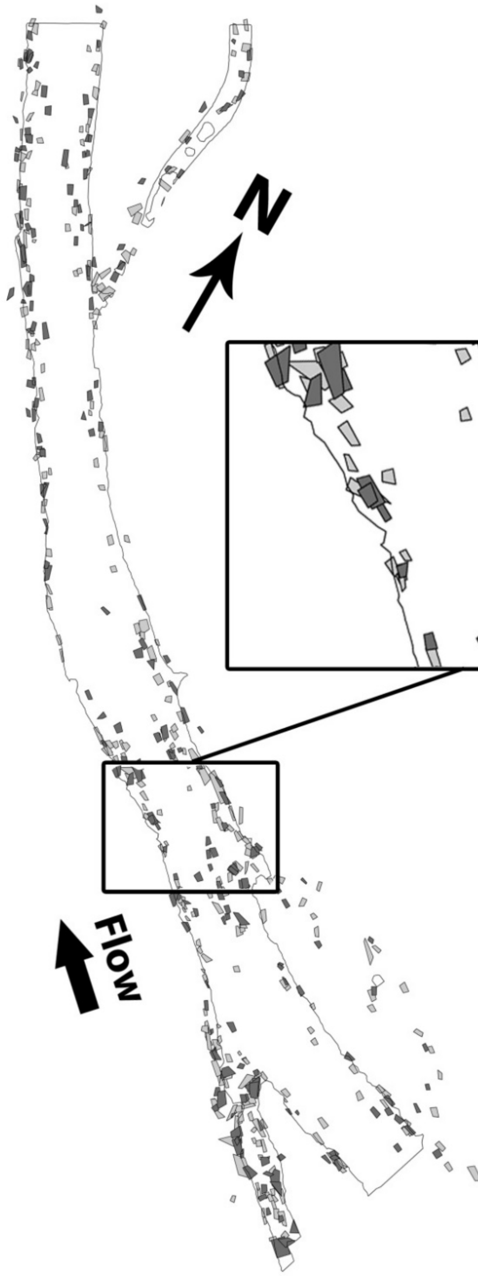

Figure 10. Example of the polygon spatial distribution at the Bucktail sampling site. Light gray polygons were created in 2013; dark gray polygons were created in 2014. The thin black line represents the wetted edge at approximate winter base flow ($8.5 m^3 s^{-1}$). Some polygons fall outside of the wetted edge when high river discharges initiate side channels and floodplain. The enlarged area shows detail.

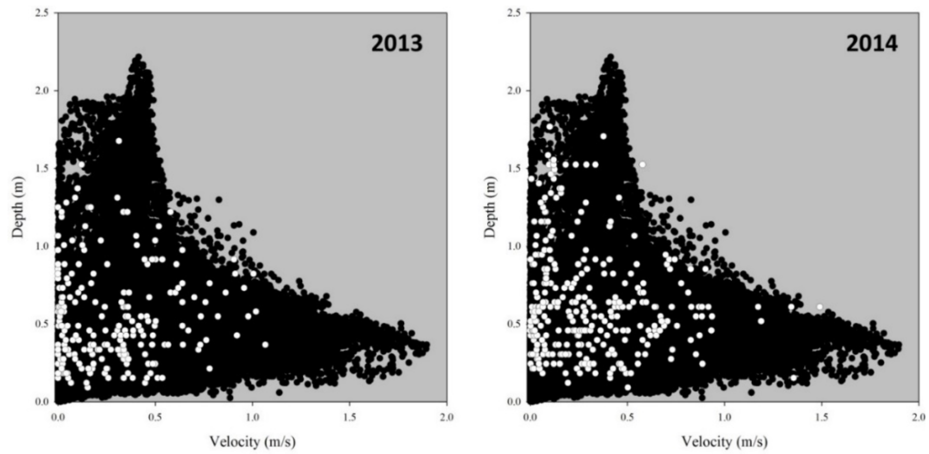

Figure 11. Distribution of sampling effort across the possible depths and velocities at the Bucktail site. Black dots are the model nodes at base flow ($8.5 m^3 s^{-1}$) with individual polygons shown as white dots. At this site there were 212 polygons surveyed in 2013 and 303 polygons surveyed in 2014.

Fish Counts

During this study there were approximately 60,000 juvenile fish counted by direct observation. Each snorkeler surveyed 128 to 781 polygons per year (Table 3). Juvenile Chinook Salmon and Coho Salmon represent the clear majority of counted juvenile fish, with relatively few juvenile steelhead trout and brown trout counted (Table 4). Although data were not recorded for non-salmonid species, snorkelers also observed other fish species, including; lamprey (*Entosphenus spp.* ammocetes, eyed juveniles, and adults), three-spined stickleback (*Gasterosteus aculeatus*), speckled dace, (*Rhinichthys osculus*), sculpin (*Cottus spp*.), and suckers (*Catostomus spp*.).

Table 3. Number of polygons surveyed per year by each snorkeler (shown here as 2-letter codes). Please note that, although not shown here, pairs of snorkelers would survey together for an entire day and attempted to snorkel together through the entire season.

	2013	**2014**
AX	292	449
AN	-	699
BR	236	759
DE	557	770
KY	304	415
LA	407	-
MA	421	128
MH	220	-
MI	159	-
NI	-	245
PA	197	281
SE	233	781
ST	365	-
TH	259	503
VI	-	360

Table 4. Number of juvenile Chinook Salmon, Coho Salmon, steelhead trout, and brown trout counted by snorkelers for 2013 and 2014 sampling seasons. Counts in the Snorkeler 1 column are from the bank-side and counts from Snorkeler 2 are the thalwag-side.

	2013		**2014**	
	Diver 1	Diver 2	Diver 1	Diver 2
Chinook < 50 mm	30285	28913	10078	9334
Chinook > 50 mm	2677	2408	3809	3731
Coho < 50 mm	1347	1309	6408	6647
Coho > 50 mm	129	151	1910	1809
Steelhead < 50 mm	138	130	1142	1001
Steelhead > 50 mm	364	207	327	318
Brown Trout < 50 mm	431	388	1113	964
Brown Trout > 50 mm	21	29	527	485

Density through Time

Fish density changed considerably between years and through the sampling seasons. In 2013, the density of juvenile Chinook Salmon was much higher than any other species (Figure 12). In 2014, mean density were similar between juvenile Chinook Salmon and Coho Salmon (Figure 12). Density of steelhead trout and brown trout was low in both years compared to salmon species. During the earliest sampling in each year, as juveniles were emerging, density was low for all species. Mid- and late-season rounds were characterized by much higher density (Figure 13), as one would expect due to cumulative emergence. In 2013, the density of each species tended to increase through all five rounds (2-6) of sampling, juvenile Chinook Salmon were present though all the sampling rounds with exceptionally high density in rounds 4-6 (Figure 13). Density of juvenile Coho Salmon, steelhead trout, and brown trout density were very low in rounds 2-3, after which density gradually increased, though remaining relatively low compared to Chinook Salmon. In 2014, with eight rounds of sampling (rounds 1-5, 7-9), mean juvenile Chinook Salmon density rose from low levels in round 1, to the highest levels in round 5, then progressively decreased in rounds 7-9 (Figure 13). Mean juvenile Coho Salmon density was low in rounds 1-3, after which levels increased in rounds 4-5, peaked in round 7, and decreased in rounds 8-9. Juvenile steelhead trout density remained at a low-level during rounds 1-5, and then increased in rounds 7-8. Juvenile brown trout density remained low in rounds 1-3, began to increase in rounds 4-5, peaked in round 7, and decreased in rounds 8-9 (Figure 13).

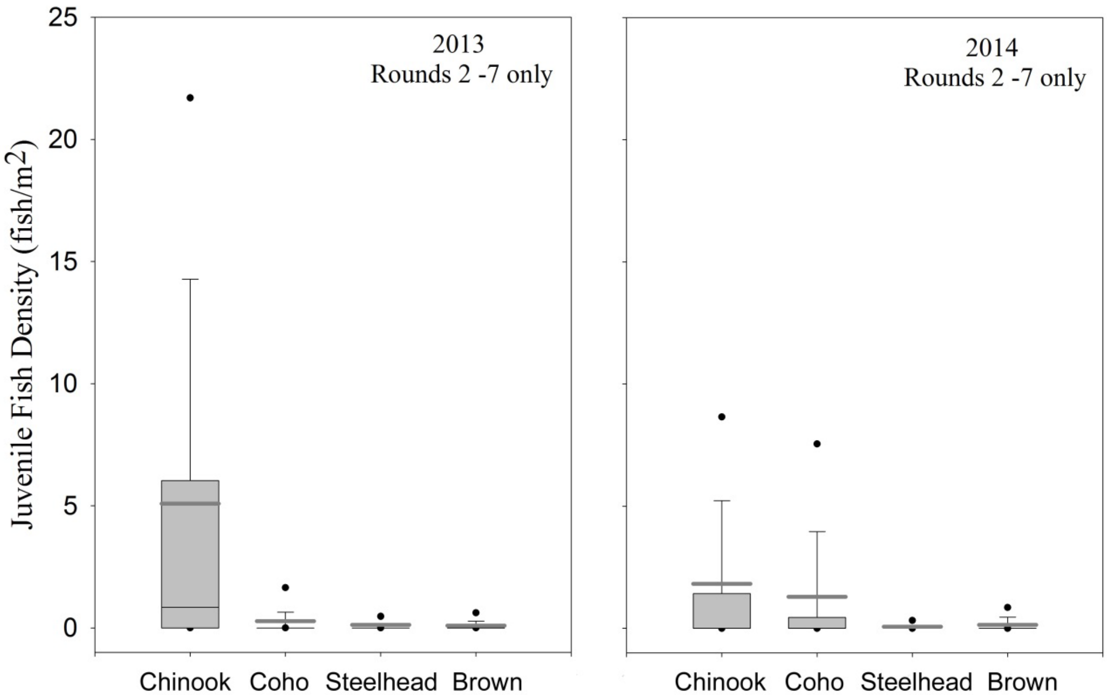

Figure 12. Range of juvenile fish density by species pooled over space and time, showing only sampling rounds 2-7 for year-to-year comparison. In these box plots the box represents the 25th and 75th percentiles, the whiskers represent the 10th and 90th percentiles, the dots represent the 5th and 95th percentiles, the thin black line is the median, and the thick gray line is the mean.

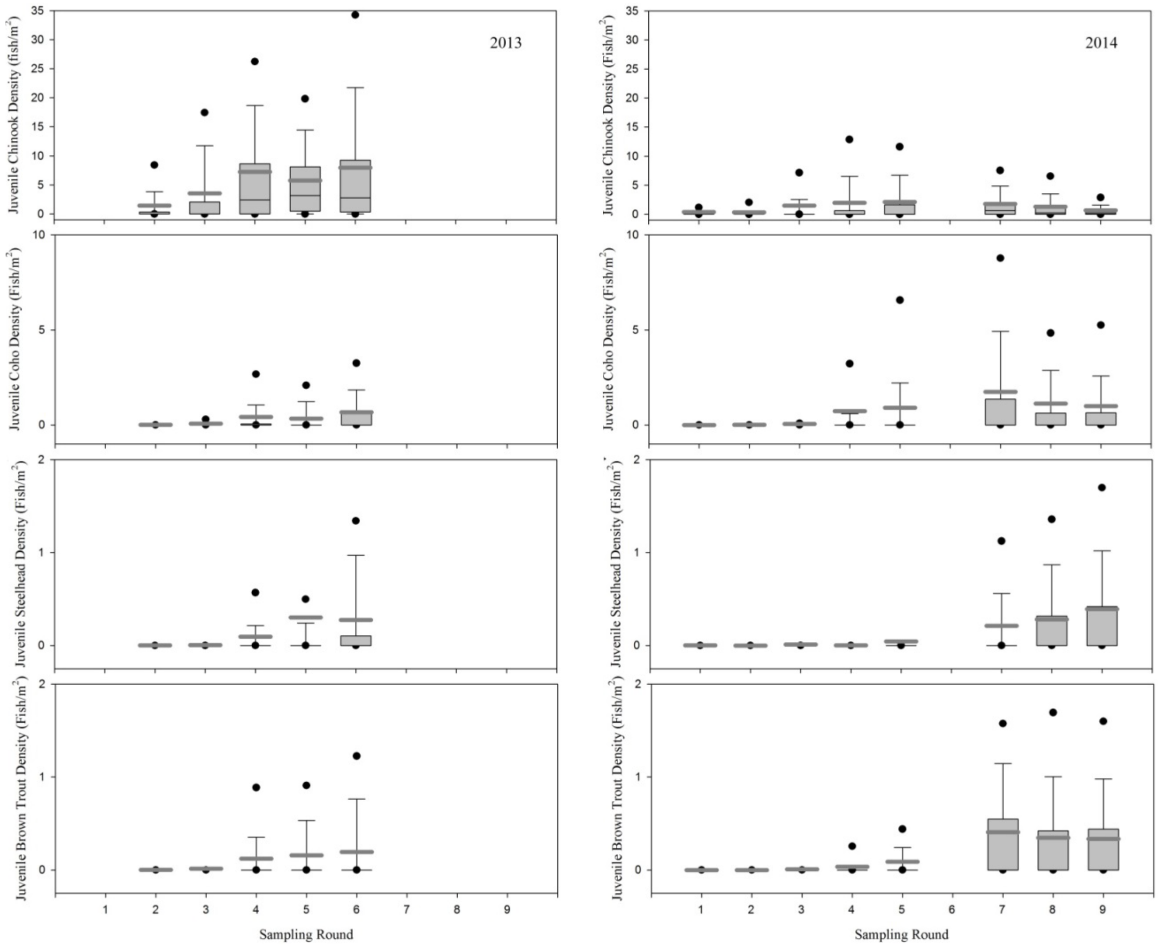

Figure 13. Range of juvenile fish density per polygon across sampling rounds (time) pooled over space. In these box plots the box represents the 25th and 75th percentiles, the whiskers represent the 10th and 90th percentiles, the dots represent the 5th and 95th percentiles, the thin black line is the median, and the thick gray line is the mean. Please note the difference in y-axis values between plots.

Density by Location

In both 2013 and 2014, the range of density of each species varied considerably across the nine sample sites (Figure 14). Juvenile Chinook Salmon mean density was highest at Cableway (2.6 km DFD), Roundhouse (46.2 km DFD), and Sheridan (48.1 km DFD). The lowest mean juvenile Chinook Salmon density was observed at McIntyre (23 km DFD). In both 2013 and 2014, the highest density of juvenile Coho Salmon was found at the most upstream site (Cableway). Overall, Coho Salmon density was higher in 2014, compared to 2013.

Juvenile steelhead trout density was highest in the upstream sites and lowest in the downstream sites in 2013. This trend then reversed in 2014, when density was highest at the downstream sites and lower at the upstream sites. Unlike the other species, brown trout density was highest in the middle sites, particularly at the Indian Creek Boat Ramp site (28.5 km DFD).

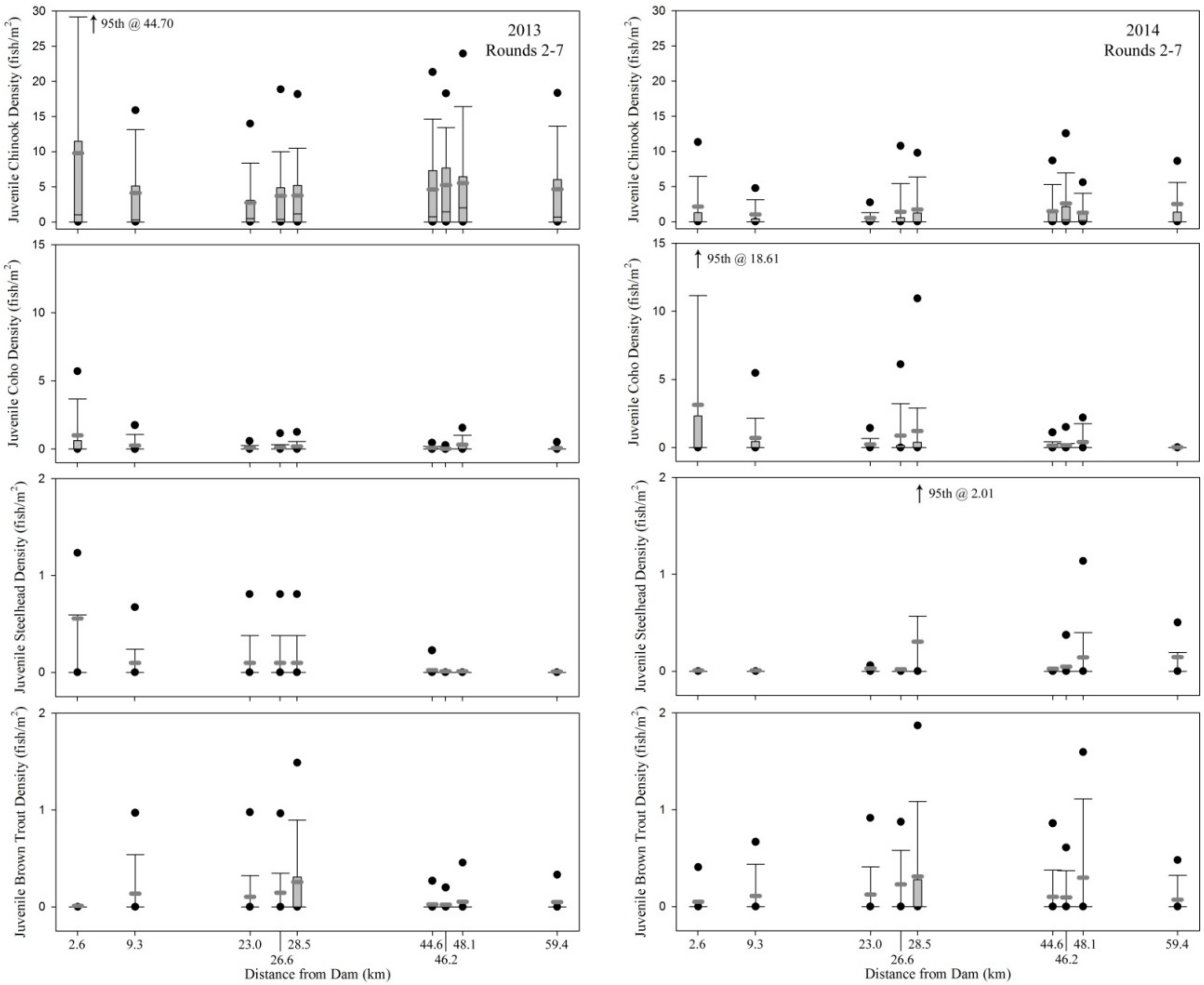

Figure 14. Range of juvenile fish density through space (shown as distance from dam) during rounds 2-7. In these box plots the box represents the 25th and 75th percentiles, the whiskers represent the 10th and 90th percentiles, the dots represent the 5th and 95th percentiles, the thin black line is the median, and the thick gray line is the mean. Please note the difference in y-axis values between plots.

Species Specific Considerations

The comparable study periods (rounds 2-7) of both years appears to have adequately captured the changes in density of Chinook Salmon and Coho Salmon from emergence through peak density. However, steelhead trout and brown trout were found at comparatively low mean density (<0.5 fish/m^2) and mostly during the late rounds in 2014, indicating that the sampling timeframe did not capture the peak of juvenile rearing for steelhead trout and brown trout.

Density by Measured Habitat Variables

Depth: Density of juvenile Chinook Salmon (Figure 15) and Coho Salmon (Figure 16) across habitat depth bins were similar within each year but differed in magnitude between years.

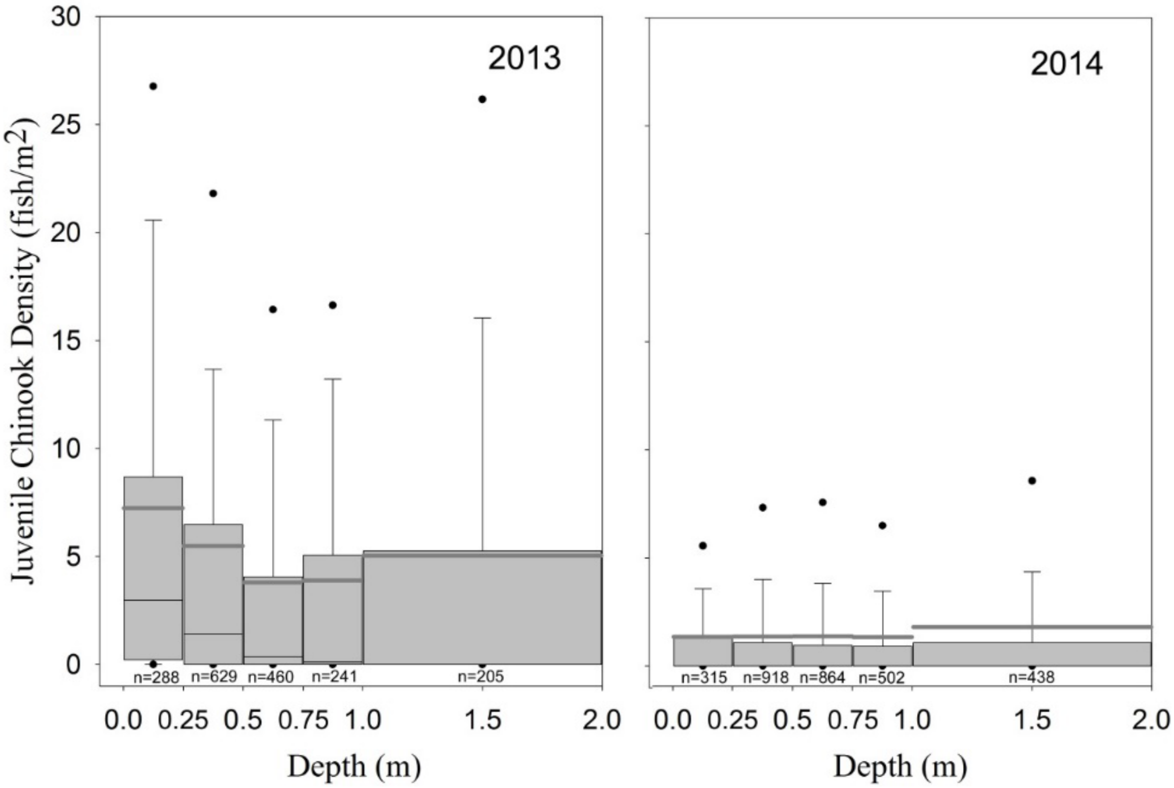

Figure 15. Range of juvenile Chinook Salmon density within depth bins for 2013 and 2014 pooled over space and time within a given year. Sample size denoted below each box plot represents the number of polygons sampled within that category. In these box plots the box represents the 25th and 75th percentiles, the whiskers represent the 10th and 90th percentiles, the dots represent the 5th and 95th percentiles, the thin black line is the median, and the thick gray line is the mean.

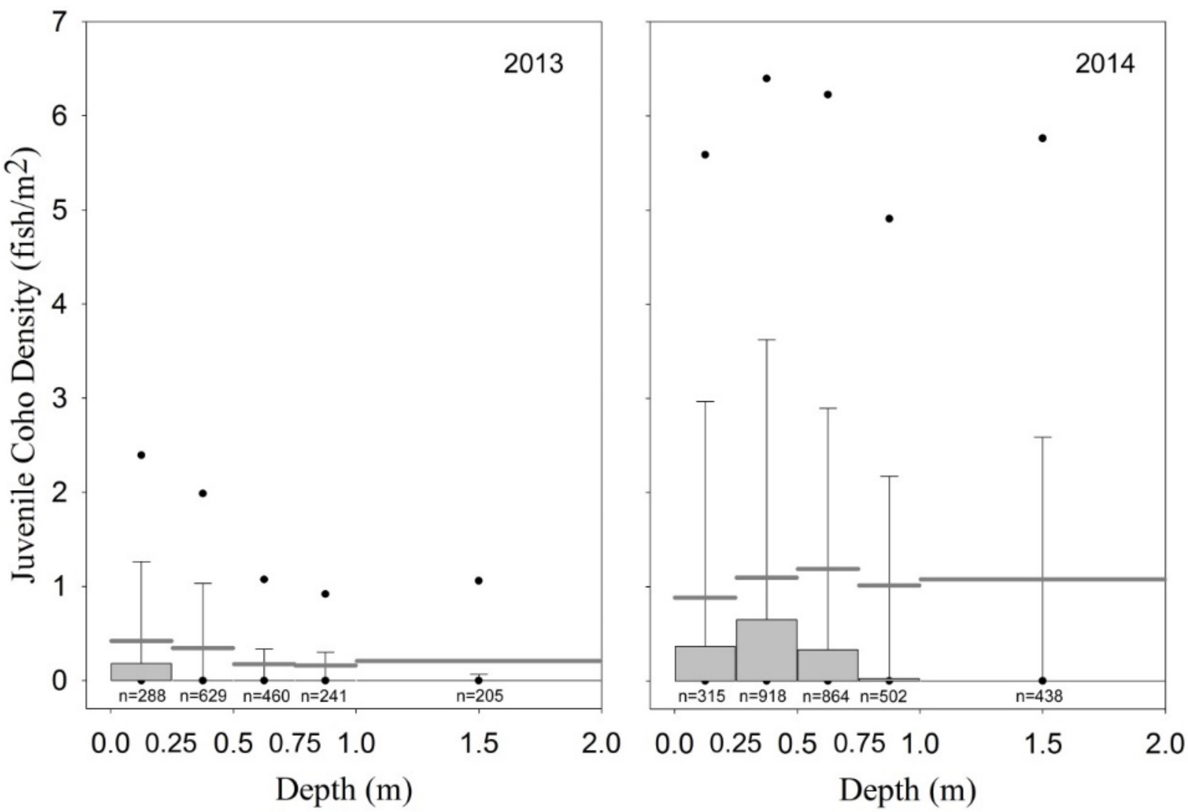

Figure 16. Range of juvenile Coho Salmon density within depth bins, pooled over space and time within a given year. Sample size denoted below each box plot represents the number of polygons sampled within that category. In these box plots the box represents the 25th and 75th percentiles, the whiskers represent the 10th and 90th percentiles, the dots represent the 5th and 95th percentiles, the thin black line is the median, and the thick gray line is the mean.

Velocity: Density of juvenile Chinook Salmon and Coho Salmon were highest in low water velocities, and dropped markedly as velocity increased from 0.0 m/s to 0.8 m/s (Figure 17 and Figure 18, respectively). This pattern was observed in both years. Juvenile fish density in water faster than 0.8 m/s were very low for juvenile Chinook Salmon and Coho Salmon.

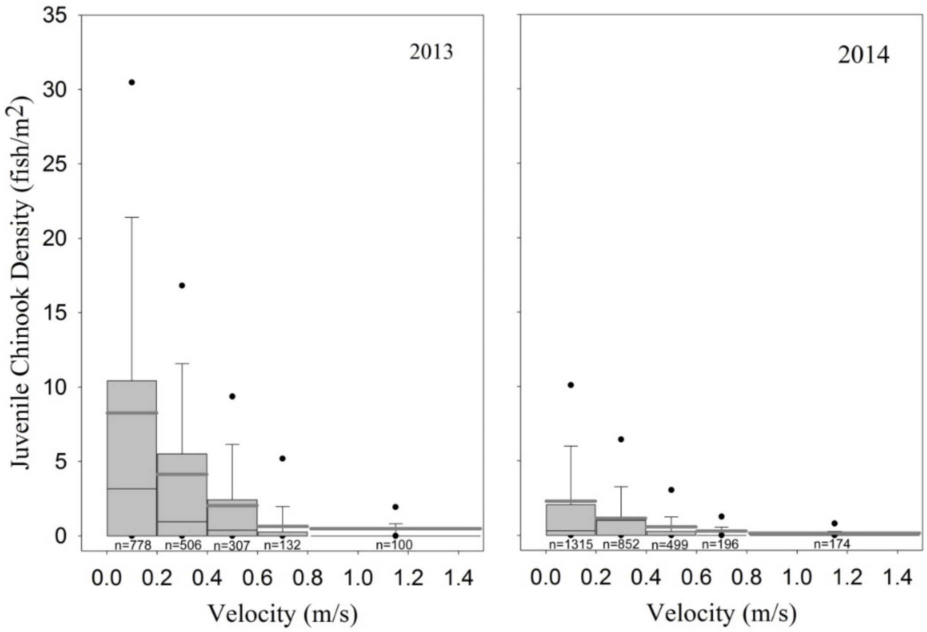

Figure 17. Range of juvenile Chinook Salmon density within water velocity bins, pooled over space and time within a given year. The sample size denoted below each box plot represents the number of polygons sampled within that category. In these box plots the box represents the 25th and 75th percentiles, the whiskers represent the 10th and 90th percentiles, the dots represent the 5th and 95th percentiles, the thin black line is the median, and the thick gray line is the mean.

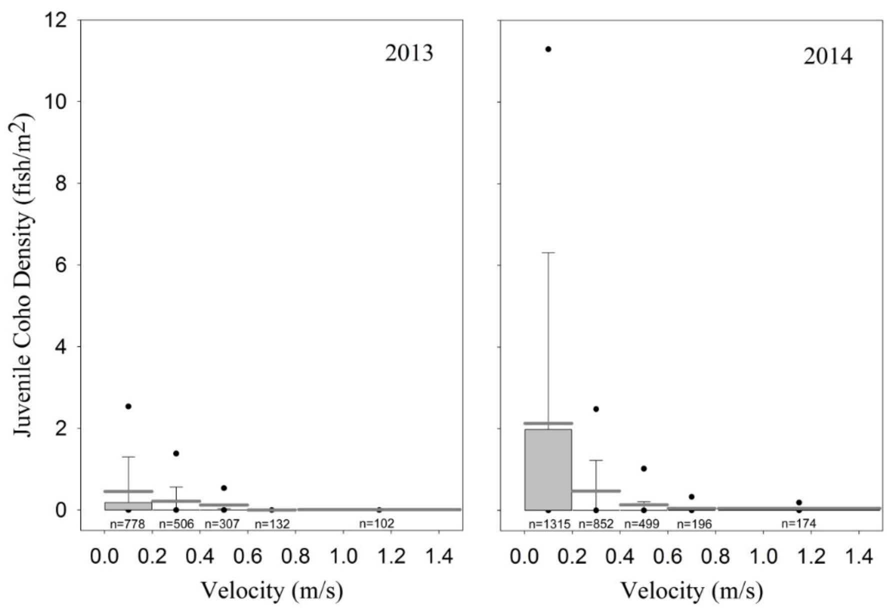

Figure 18. Range of juvenile Coho Salmon density within water velocity bins, pooled over space and time within a given year. The sample size denoted below each box plot represents the number of polygons sampled within that category. In these box plots the box represents the 25th and 75th percentiles, the whiskers represent the 10th and 90th percentiles, the dots represent the 5th and 95th percentiles, the thin black line is the median, and the thick gray line is the mean.

Adjacent Velocity: Density of juvenile Chinook Salmon and Coho Salmon did not appear to be affected by adjacent velocity in 2013 (Figure 19), but in 2014 showed a slight increase in density in polygons with higher reference velocity and larger difference in adjacent velocity (Figure 20). Coho Salmon density did not appear to be affected by adjacent velocity (Figure 21).

Side Channel: To evaluate mainstem and side channel data equally, all polygons with high depth and/or velocity were removed (as these features are very rare and/or absent from side channels). Cableway, Bucktail, McIntyre, and Indian Creek Side Channel sites contain side channels and were evaluated. Data pooled over time did not show a consistent species-specific pattern between sites for juvenile Chinook Salmon and Coho Salmon (Figure 22), but suggested that within site there may have been partitioning based on species (i.e., juvenile Chinook Salmon were found at Cableway in higher density in the mainstem compared to the side channel, whereas Coho Salmon showed the opposite pattern).

Substrate: In general, density of juvenile Chinook Salmon and Coho Salmon was higher in polygons with small substrate and lower in polygons with large substrate (Figure 23). Juvenile Chinook Salmon density was highest in both silt and sand substrates, while gravel, cobble, boulder, and bedrock generally exhibited similar density ranges. Density of juvenile Coho Salmon was highest in silt and decreased as substrate size increased. These data were only collected in 2014.

Distance to Cover: Density of juvenile Chinook Salmon and Coho Salmon were highest in polygons that were close to cover (Figure 24 and Figure 25). The relationship between juvenile Chinook Salmon density and distance to cover decreases up to 6 m from cover in 2013 and 8 m in 2014, and then appears to be unrelated to distance from cover beyond these distances. Similarly, juvenile Coho Salmon density appear to have a declining strong relationship with distance to cover, but up to 6 to 8 m, beyond which density appears to be unrelated to distance from cover.

Cover Type: Density of juvenile Chinook Salmon and Coho Salmon were greater in all cover types compared to polygons without cover, with the exception of aquatic vegetation (Figure 26 and Figure 27). It is difficult to discern a relationship between fish density and cover type. Some cover types (grasses, blackberry, and horsetail) are only available to juvenile salmon when they are inundated by ROD flows which coincides with when density of juvenile Chinook Salmon and Coho Salmon were highest.

Cover Density: Density of juvenile Chinook Salmon and Coho Salmon were higher in polygons with high density cover and lower in polygons with low cover density or no cover (Figure 28). The trend of higher juvenile salmon density in higher cover density is slightly stronger for juvenile Coho Salmon, compared to juvenile Chinook Salmon. These data were only collected in 2014.

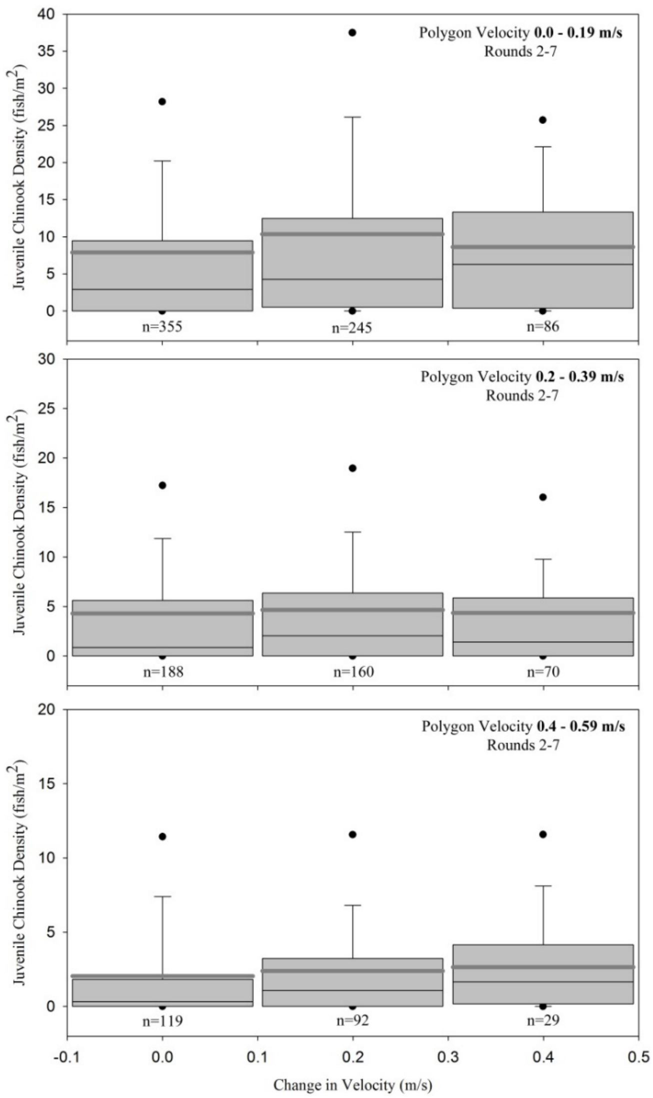

Figure 19. Range of juvenile Chinook Salmon density within change in velocity ($velocity_{adjacent}$ – $velocity_{representative}$) bins, separated into three polygon velocity groups, pooled over space and time (2013; rounds 2-7 only). The sample size denoted below each box plot represents the number of polygons sampled within that category. In these box plots the box represents the 25th and 75th percentiles, the whiskers represent the 10th and 90th percentiles, the dots represent the 5th and 95th percentiles, the thin black line is the median, and the thick gray line is the mean.

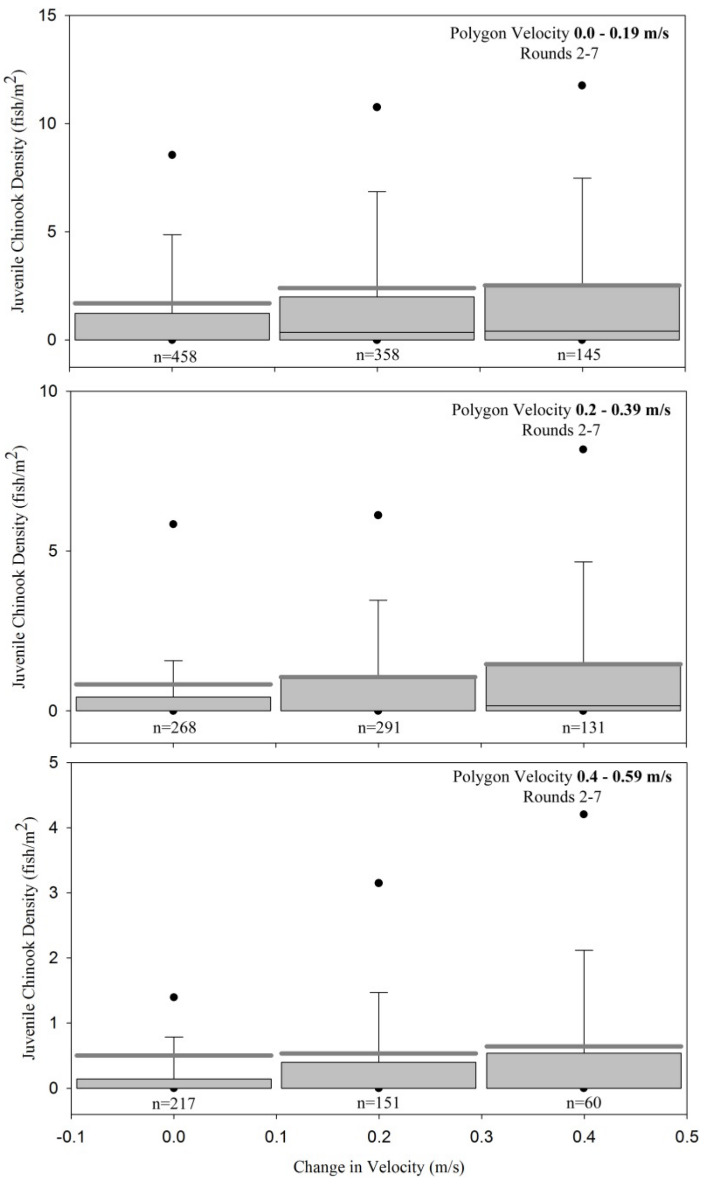

Figure 20. Range of juvenile Chinook Salmon density within change in velocity ($velocity_{adjacent} - velocity_{representative}$) bins, separated into three polygon velocity groups, pooled over space and time (2014; rounds 2-7 only). The sample size denoted below each box plot represents the number of polygons sampled within that category. In these box plots the box represents the 25th and 75th percentiles, the whiskers represent the 10th and 90th percentiles, the dots represent the 5th and 95th percentiles, the thin black line is the median, and the thick gray line is the mean.

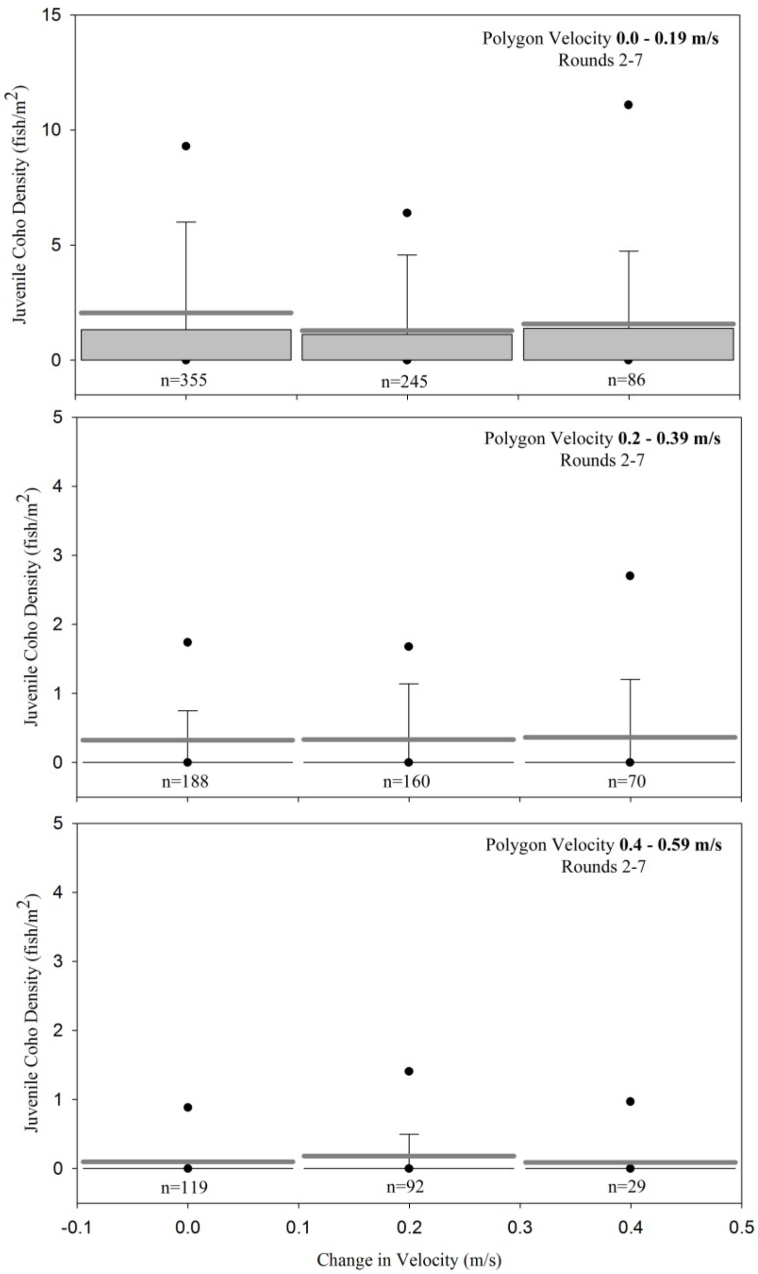

Figure 21. Range of juvenile Coho Salmon density within change in velocity ($velocity_{adjacent}$ – $velocity_{representative}$) bins, separated into three polygon velocity groups, pooled over space and time (2014; rounds 2-7 only). The sample size denoted below each box plot represents the number of polygons sampled within that category. In these box plots the box represents the 25th and 75th percentiles, the whiskers represent the 10th and 90th percentiles, the dots represent the 5th and 95th percentiles, the thin black line is the median, and the thick gray line is the mean.

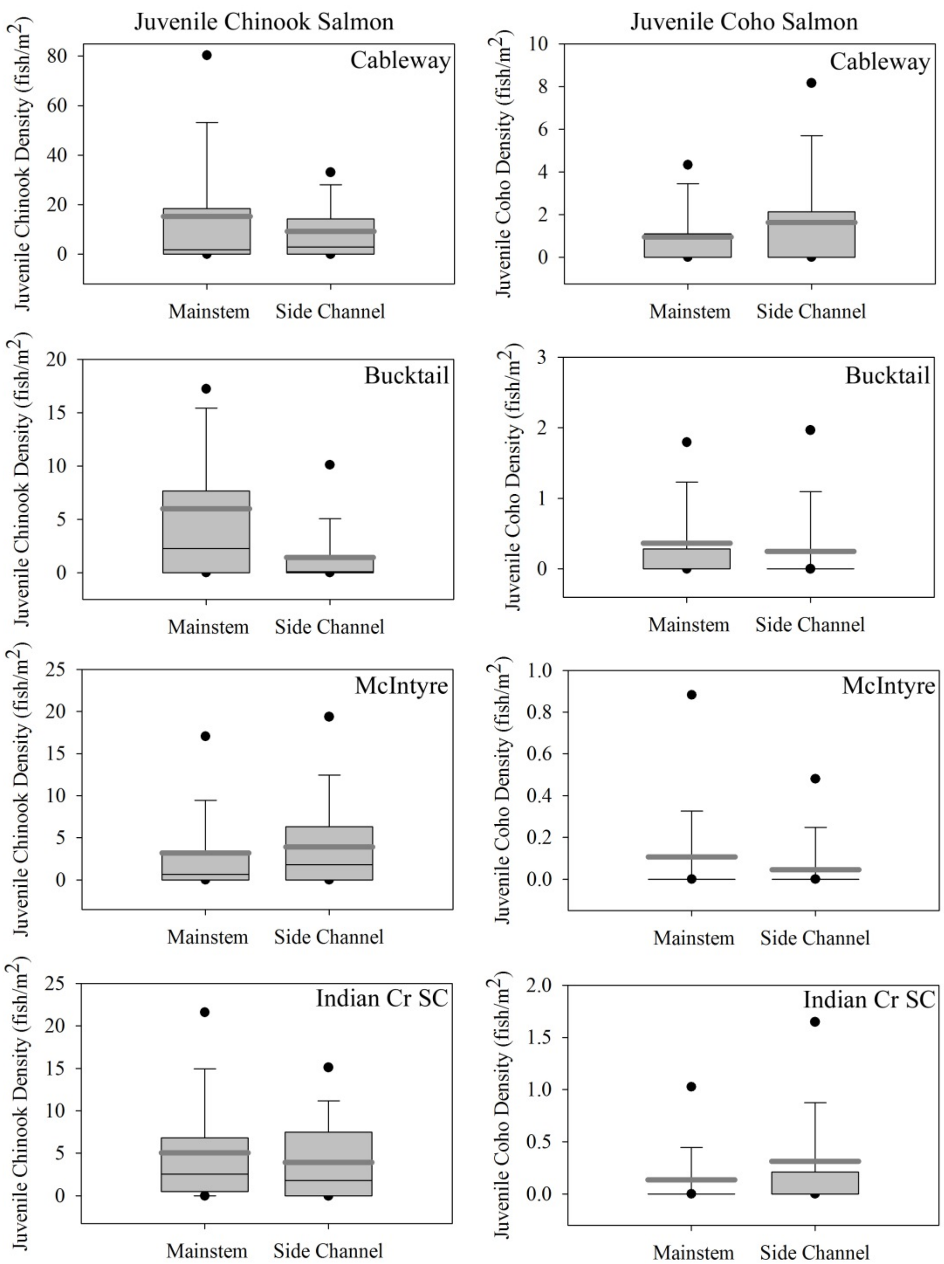

Figure 22. Range of juvenile Chinook Salmon and Coho Salmon density within mainstem and side channel habitats, pooled over space and time, 2013. Data from high velocity and/or depths were removed from both categories, as they are uncommon or absent from most side channel habitats. In these box plots the box represents the 25th and 75th percentiles, the whiskers represent the 10th and 90th percentiles, the dots represent the 5th and 95th percentiles, the thin black line is the median, and the thick gray line is the mean.

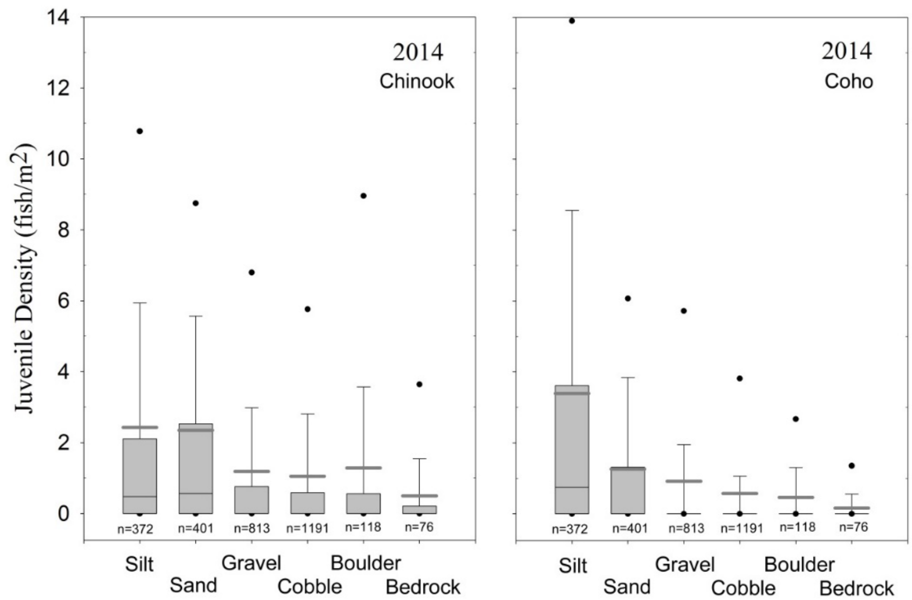

Figure 23. Range of juvenile Chinook Salmon and Coho Salmon density by dominate polygon substrate type in 2014, pooled over space and time. The sample size denoted below each box plot represents the number of polygons sampled within that category. In these box plots the box represents the 25th and 75th percentiles, the whiskers represent the 10th and 90th percentiles, the dots represent the 5th and 95th percentiles, the thin black line is the median, and the thick gray line is the mean.

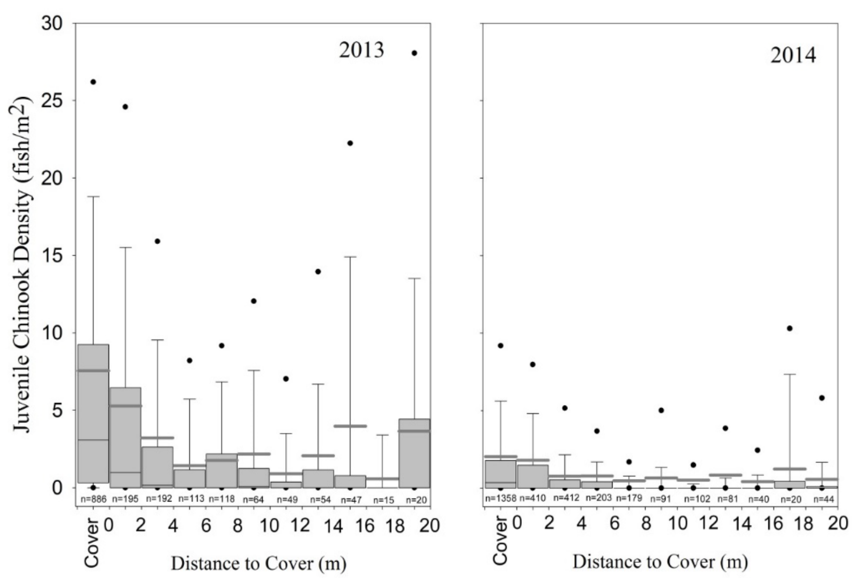

Figure 24. Range of juvenile Chinook Salmon density within distance to cover bins, pooled over space and time within a given year. The sample size denoted below each box plot represents the number of polygons sampled within that category. In these box plots the box represents the 25th and 75th percentiles, the whiskers represent the 10th and 90th percentiles, the dots represent the 5th and 95th percentiles, the thin black line is the median, and the thick gray line is the mean.

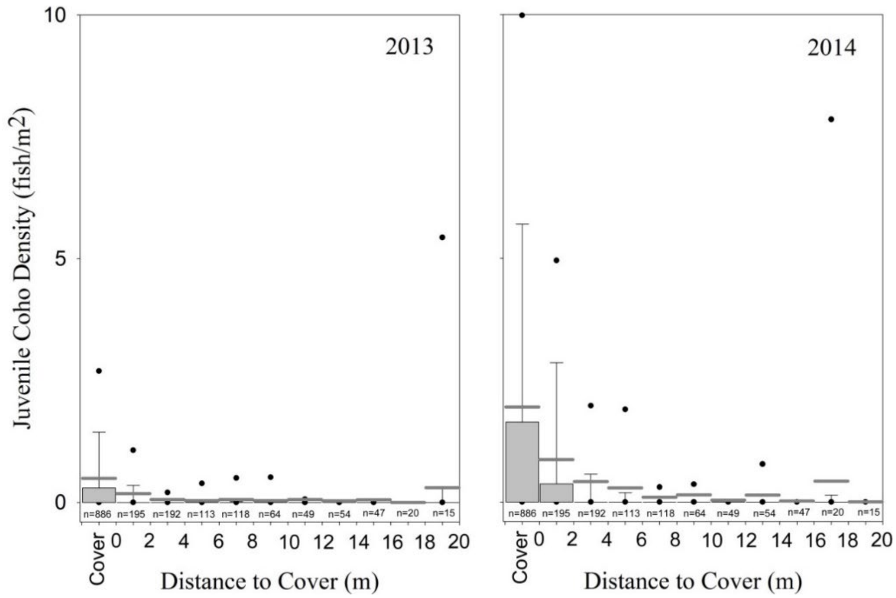

Figure 25. Range of juvenile Coho Salmon density within distance to cover bins, pooled over space and time within a given year. The sample size denoted below each box plot represents the number of polygons sampled within that category. In these box plots the box represents the 25th and 75th percentiles, the whiskers represent the 10th and 90th percentiles, the dots represent the 5th and 95th percentiles, the thin black line is the median, and the thick gray line is the mean.

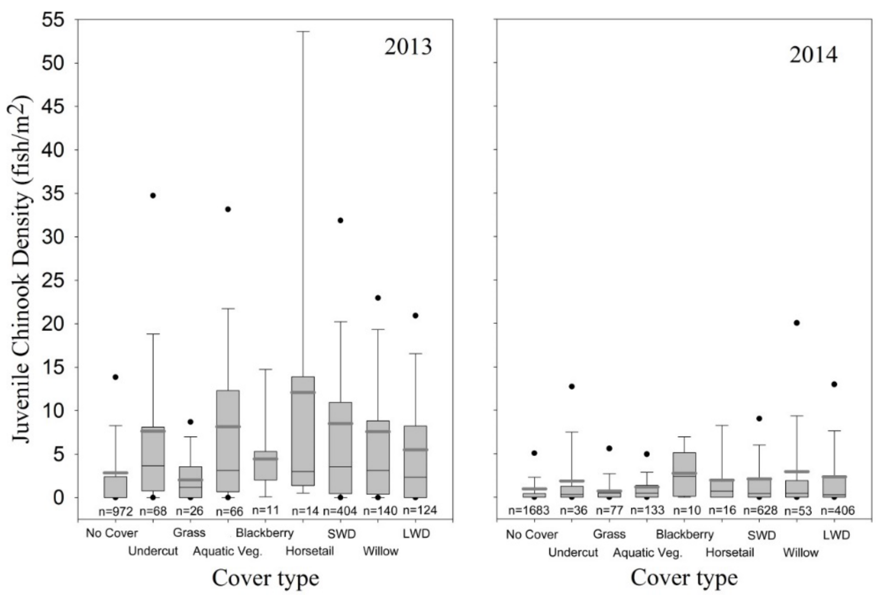

Figure 26. Range of juvenile Chinook Salmon density by cover type, pooled over space and time within a given year. The sample size denoted below each box plot represents the number of polygons sampled within that category. In these box plots the box represents the 25th and 75th percentiles, the whiskers represent the 10th and 90th percentiles, the dots represent the 5th and 95th percentiles, the thin black line is the median, and the thick gray line is the mean.

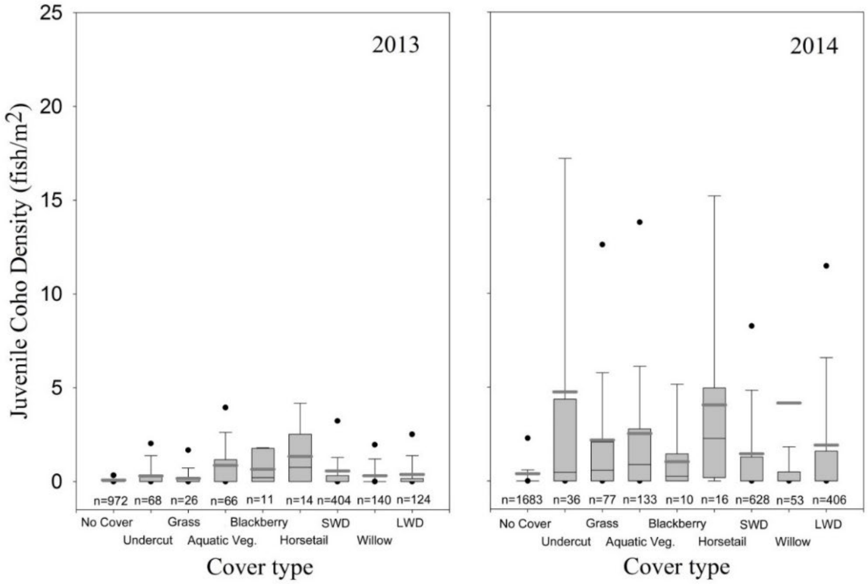

Figure 27. Range of juvenile Coho Salmon density by cover type, pooled over space and time within a given year. The sample sizes denoted below each box plot represents the number of polygons sampled within that category. In these box plots the box represents the 25th and 75th percentiles, the whiskers represent the 10th and 90th percentiles, the dots represent the 5th and 95th percentiles, the thin black line is the median, and the thick gray line is the mean.

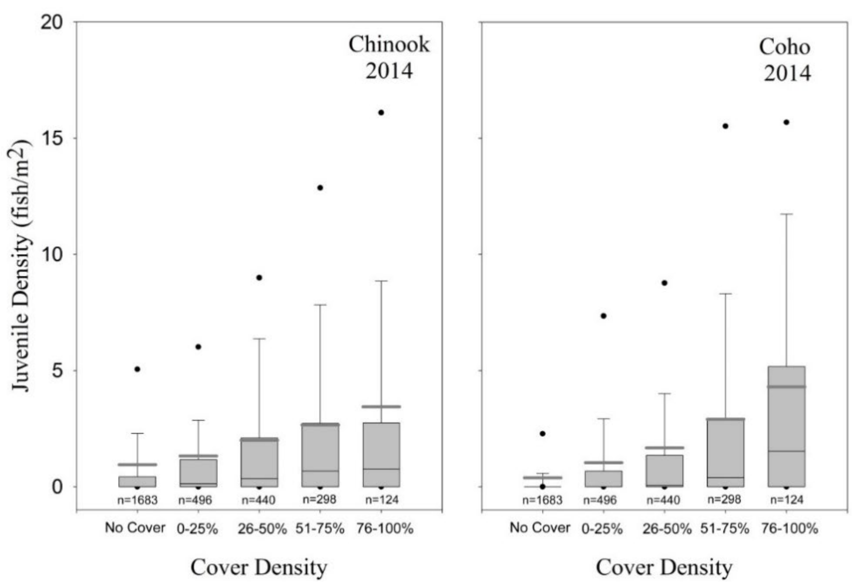

Figure 28. Range of juvenile Chinook Salmon and Coho Salmon density within cover density bins in 2014, pooled over space and time. The sample sizes denoted below each box plot represents the number of polygons sampled within that category. In these box plots the box represents the 25th and 75th percentiles, the whiskers represent the 10th and 90th percentiles, the dots represent the 5th and 95th percentiles, the thin black line is the median, and the thick gray line is the mean.

Distance to Bank: Density of juvenile Chinook Salmon and Coho Salmon were highest in polygons that were closest to the bank (Figure 29). Juvenile Chinook Salmon appear to have a relationship with distance to bank out to 14 m, while juvenile Coho Salmon appear to maintain this relationship out to only 8 m. These data were only collected in 2014.

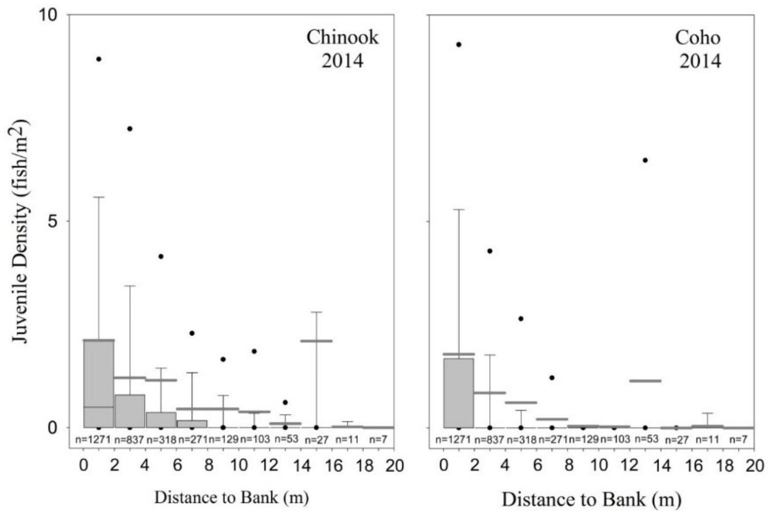

Figure 29. Range of juvenile Chinook Salmon and Coho Salmon density within distance to bank bins in 2014, pooled over space and time. The sample size denoted below each box plot represents the number of polygons sampled within that category. In these box plots the box represents the 25th and 75th percentiles, the whiskers represent the 10th and 90th percentiles, the dots represent the 5th and 95th percentiles, the thin black line is the median, and the thick gray line is the mean.

Statistical Model Selection and Fitting

Like Miller et al. (2011), two phases of model building and estimation were conducted. First, in the model selection phase, parameters were estimated using maximum likelihood techniques and the weight of evidence for including potential covariates was calculated over space (site) and time (round). In the second phase, inference and estimation were conditioned on the spatial and temporal effects to isolate the effects of physical habitat characteristics retained in model selection. In the second phase, a Bayesian implementation of the model was conducted to infer the importance of each of the physical habitat characteristics.

The full set of covariates for the *zero-inflation* component of the model included distance to cover, depth, and velocity, with each interacting with temporal effects. In addition, the full set of covariates considered for the *abundance* component of the model included distance to cover, depth, and velocity, as well as quadratic terms for each and all 2-way interactions among the three physical variables. Finally, the full set of covariates considered for the *detection component* of the model included individual snorkeler effects, depth, visibility, and a temporal (round) effect. The model selection process resulted in an optimal model defined here as the *inference model*. Compared to the full set of covariates considered, the inference model did not include the visibility term of the detection component of the model, nor any of the interaction terms from the zero-inflated component, however, all abundance covariates remained.

In the second phase, the parameters of the inference model were calculated using Bayesian Markov-Chain Monte Carlo (MCMC) methods. The likelihood and specified prior distributions were constructed using BUGS language and called JAGS (Plummer 2014) from R via the package jagsUI (Kellner 2014) to simulate MCMC draws from the joint posterior distribution of all parameters. Mean-zero vague Gaussian priors were specified for all regression coefficients, and vague uniform priors were specified for all temporal and spatial random effect variance components (Gelman 2006). Three MCMC chains were run and 3,000 samples per chain were retained. Goodness-of-fit (Kery and Schaub 2012, p. 402) and MCMC convergence (Gelman et al. 2014) were assessed using standard methods, and justified confidence in modeling results.

Posterior distribution estimates indicated that detection probability decreased with increasing depths and among snorkelers (Table 5: Detection), with average snorkeler detection rate estimates ranging from 0.76 to 0.92. Posterior distribution estimates also suggested that physical variables were associated with the presence and abundance of juvenile Chinook Salmon at the sampling locations. The probability of a site containing any juvenile Chinook Salmon at all decreased with increasing water depth, velocity, and distance to cover (Table 5: Zero-Inflation). Given juvenile Chinook Salmon were present, the posterior distributions suggested that abundances decreased with increasing distance from escape cover (Table 5: Abundance). Whereas there was posterior evidence suggesting that increasing velocities lead to decreased abundances, the role of water depth appears to mitigate the effects of increasing mean column velocities in deeper sections, rather than directly relate to local abundances (Table 5: Abundance). In general, there was much less posterior evidence that other interactions and the quadratic terms were associated with variation in local abundances (Table 5: Abundance).

Table 5. Summaries of fixed-effects parameter posterior densities, separated by the zero-inflation, Poisson mean, and detection probability components of our model. Point estimates (Mean) represent posterior distribution means, and the lower (LCL) and upper limits (UCL) of 95% credible intervals were created using the 0.025 and 0.975 quantiles of posterior distribution values. Rhat represents values of the Gelman-Rubin diagnostic to evaluate convergence among multiple MCMC chains. "D2Cover" abbreviates the distance to cover covariate. A "^{2}" superscript represents a quadratic coefficient, and ":" indicates a coefficient for the interaction of covariates. All reported values are on the scale of their respective link function. The interested reader can find variance component parameter estimates in the companion manuscript.

Parameter	Mean	LCL	UCL	Rhat
Zero-Inflation				
Intercept	1.14	-1.30	3.69	1.01
Velocity	-0.88	-1.08	-0.67	1.00
Depth	-0.73	-0.91	-0.56	1.00
D2Cover	-0.52	-0.68	-0.36	1.00
Abundance				
Intercept	-1.86	-2.60	-1.19	1.02
Velocity	-0.68	-0.85	-0.52	1.00
Depth	0.01	-0.14	0.16	1.00
D2Cover	-0.68	-0.91	-0.44	1.00
Depth2	0.05	-0.02	0.13	1.00
Velocity2	-0.01	-0.12	0.11	1.00
D2Cover2	0.14	0.06	0.23	1.00
Depth:Velocity	0.20	0.04	0.37	1.00
Velocity:D2Cover	0.06	-0.10	0.23	1.00
Depth:D2Cover	-0.12	-0.31	0.08	1.00
Detection				
Intercept	1.20	0.81	1.60	1.00
Diver2	0.75	0.29	1.21	1.00
Diver3	1.17	0.85	1.49	1.00
Diver4	1.22	0.82	1.61	1.00
Diver5	1.07	0.67	1.47	1.00
Diver6	1.04	0.70	1.37	1.00
Diver7	1.01	0.65	1.37	1.00
Diver8	0.46	0.02	0.92	1.00
Diver9	1.10	0.68	1.51	1.00
Diver10	1.14	0.65	1.63	1.00
Diver11	1.23	0.87	1.57	1.00
Diver12	0.29	-0.12	0.71	1.00
Depth	-0.26	-0.38	-0.13	1.00

DISCUSSION

The goal of this project was to develop a model that would tie juvenile salmon density to physical habitat characteristics. Distributing sampling over a wide range of physical habitat characteristics allows development of habitat to fish density relationships that will be explored in a companion manuscript detailing analyses of all explanatory variables in various combinations, as noted above.

The stratified random sampling design was successful in distributing sample locations through the 2-D sites and across a wide range of depth and velocities. Further, the data obtained from our sampling design led to our ability to observe patterns in fish density related to contrasting levels of habitat depths, velocities, and distances to cover. Sampling in very shallow water is difficult for snorkels and few polygons were sampled in <0.1 m deep water and may have been underrepresented in our data; we feel this is a relatively small proportion of possible polygons and does not bias the results of the shallowest bin. However, sampling in water deeper than 1.83 m was purposely removed from the survey, as it is too deep for accurate snorkeler-based fish counts, and our estimates of density in deep bins may be biased low.

The specific location of the nine 2-D sites was predetermined before this study. From the data it appears that there is a non-linear and variable relationship between RKM and fish density. This relationship may have become clearer if sample locations between Bucktail and McIntyre or Indian Creek Side Channels and Evans Bar existed.

Snorkeling

Snorkelers were well trained and adept at locating and identifying juvenile salmonids. All snorkeling in this study occurred during daylight hours, because in a previous study (Pinnix et al. 2016) snorkeling was conducted both day and night and did not find significant differences in site level density between day and night for both Chinook Salmon and Coho Salmon. However, both species were utilizing cover during daylight hours and spread out evenly over the bottom, not associated with cover, during night hours. Therefore, we felt that daylight surveys for juvenile Chinook Salmon and Coho Salmon were valid and more useful in a management context when considering restoration actions that seek to build complexity and cover for juvenile salmon that are utilizing these features. In contrast, we feel that surveys for steelhead trout and brown trout should be conducted during nighttime hours due to their more nocturnal lifestyle and affinity for crevices between substrate during daylight hours.

Effects of Weather & Flows

Precipitation during the 2013 and 2014 sampling seasons was below average and may have had several effects on this study. Positive effects may have included low turbidity leading to high snorkeler detection estimates (0.76 – 0.92), few missed sampling opportunities due to storm events, and consistent flows between polygon setup and snorkeling survey. Negative effects may include early emergence timing and dispersal of juveniles which would affect habitat availability, as the low flows resulting from below average rainfall may have limited the amount and types of cover available in the river channel.

Time (Sampling Rounds)

The time frame of this study appears to adequately capture the density of juvenile Chinook Salmon and Coho Salmon across their emergence and early rearing period, including the period of peak density. The sampling period however, was not designed to capture the rearing period of steelhead trout and brown trout. The 2013 sampling appears to encompass the emergence of all salmonid species but may have ended prior to peak abundance. The 2014 sampling, which started earlier and ended later, appears to have included the emergence, peak abundance, and dispersal of juvenile Chinook Salmon, Coho Salmon, and brown trout, but not steelhead trout. Juvenile Chinook Salmon were the earliest to emerge in both 2013 and 2014. Emergence for juvenile Coho Salmon, steelhead trout, and brown trout seemed to happen within the same time frame, except for steelhead trout in 2014, which emerged much later. Peak density of juvenile Coho Salmon, steelhead trout, and brown trout all occurred several weeks later than juvenile Chinook Salmon.

Location (Site, RKM)

The relationship between juvenile salmon density and river kilometer is not linear. That is, there are areas of higher density along the longitudinal gradient that is unrelated to distance from the dam. This could be due in part to location of spawning. For instance, in recent years, between 83% and 87% of adult spawners have spawned within 10 km of Lewiston Dam (Rupert et al. 2017) and Cableway, our sample site closest to the dam, contains the highest density of Chinook Salmon and Coho Salmon. However, location of spawning is unlikely to describe all the variation in juvenile density, as we know that juvenile salmon disperse after hatching and rear in different habitats on their seaward migration.

There is likely an interaction between time (sample round) and river kilometer, because as fish grow (and time progresses) fish migrate downstream. Our initial summary of the data here was unable to tease out this interaction effect, that we hope will be more apparent in future analyses that are more rigorous.

Measured Variables

Nearly all habitat metrics collected for each polygon appear to provide important insights into the range of density at which juvenile salmonids occupy habitats in the Trinity River. Strongest of these appears to be water velocity. Interactions likely exist between water velocity and other measured variables, such as substrate, distance to bank, distance to cover, and density of cover. For example, silt and sands are likely rare in high water velocities due to increased sheer stress.

Generally, the mean density of juvenile Chinook Salmon and Coho Salmon increase as the size of the dominant substrate decreases (Figure 23). The relationship between substrate and fish density are likely due to co-variation with velocity.

The relationship between density of juvenile Chinook Salmon and distance to cover was an important parameter in zero-inflation and abundance portions of the statistical model. This finding is not unexpected, however, it appears that the relationship is strongest for Chinook Salmon out to 6m (Figure 24) and out to 4m for Coho Salmon (Figure 25). Distance to the bank seems to have an effect on both juvenile Chinook Salmon and Coho Salmon (Figure 29), although this measure was not kept in the optimal statistical model. It appears that juvenile Coho Salmon density declines faster as distance to bank increases than that of juvenile Chinook Salmon. Similarly, it appears that juvenile Coho Salmon have more preference for the higher density cover, than juvenile Chinook Salmon.

Comparisons to IHAP

The integrated habitat assessment plan (IHAP), that uses habitat guilds to describe where fish are most abundant, was supported by the robust dataset collected during this study (Goodman et. al 2010). The IHAP method for evaluating juvenile rearing habitat uses depth (fry: <2.0ft, presmolt: <3.0ft), velocity (fry: <0.4ft/s, presmolt: <0.8ft/s) and presence/absence of cover as the sole habitat criteria. These three variables provide a broad and consistent view of habitat that can be measured to provide insight into pre- and post-restoration activities. Our finding here generally supports the IHAP habitat guilds (Figure 30), especially the zero-inflation portion of the model that predicts presence or absence of juvenile salmonids based on depth, velocity and distance to cover. However, the abundance portion of the model also included quadratic terms and interaction terms that show a more complex picture of the distribution of juvenile Chinook Salmon. While the IHAP guilds do a good job of determining whether juvenile salmonids may be present or not, they do not provide much insight into finer-scale characteristics that determine the density of juvenile salmonids.

Statistical Model Use in Stream Salmonid Simulator (SSS)

As noted above, this project was initiated with the precise goal of estimating the association of fish abundance (or density) with physical habitat characteristics to inform the SSS Chinook Salmon population dynamics model. Habitat availability is often expressed in population dynamics models via a habitat suitability index (HSI). HSI values range between 0 (lower bound representing least unsuitable habitat) and 1 (upper bound representing the most suitable habitats). The probability distribution (zero-inflated Poisson) employed in our statistical modeling makes HSI implementation very straightforward. By incorporating the posterior variation for each parameter, the generated HSI values can even reflect the parameter uncertainty of our model. For a given set of physical variable values, given model parameter estimates, the probability of any count arising stochastically can be calculated. A natural HSI measure in this context is 1 – probability (abundance = 0). If the estimated probability of abundance being zero is very high, that would indicate relatively poor habitat quality. Conversely, if the estimated probability of abundance being zero is very low, that would indicate relatively high habitat quality.

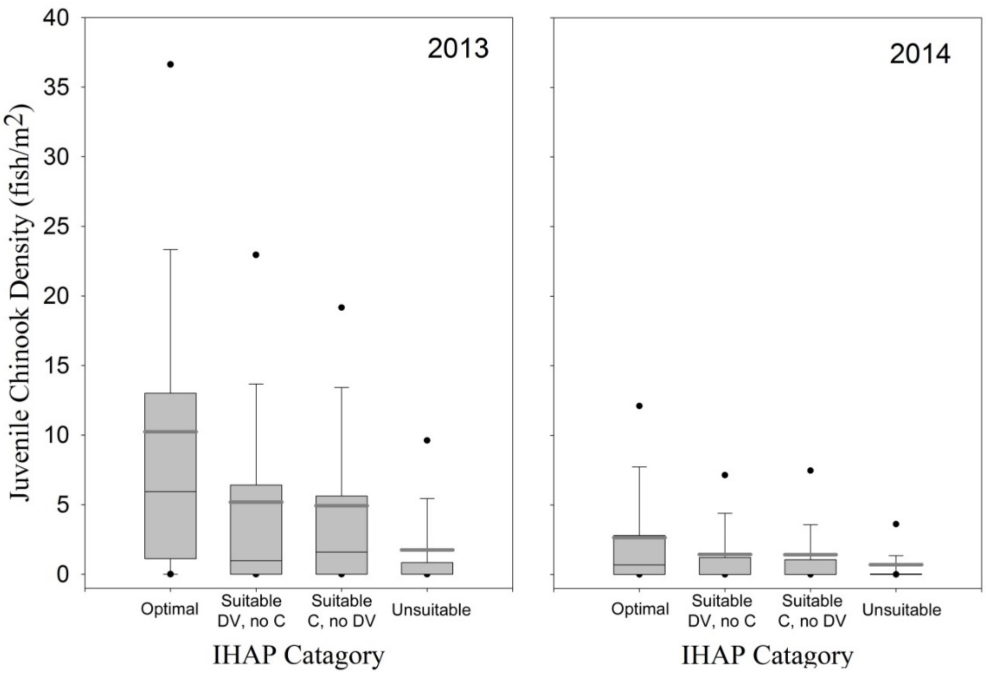

Figure 30. Range of juvenile Chinook Salmon density within the Integrated Habitat Assessment Plan habitat categories (Goodman et al., 2010), pooled over space and time within a given year. Even though the magnitude is substantially different between the two years, the relationship between the categories appears to remain (i.e., high, moderate, moderate, low), and this relationship is very similar to the study by Goodman et al. (2010). In these box plots the box represents the 25th and 75th percentiles, the whiskers represent the 10th and 90th percentiles, the dots represent the 5th and 95th percentiles, the thin black line is the median, and the thick gray line is the mean.

Conclusion

This project provided valuable information for the development and parameterization of the SSS model. Our findings here also helped to further validate the IHAP habitat guilds However, we demonstrated finer scale characteristics determining the density of juvenile salmonids and showed there are additional subtleties to the optimal habitats that fish occupy within the IHAP guilds.

ACKNOWLEDGEMENTS

We would like to thank the hard work of the technicians that worked on this project: Matt Drummond (USFWS), Andrew Goodman (USFWS), Brian Jordan (HVF), Seth Brenton (HVT), Thomas Maston (HVT), Nick Davids (YTF), Axle Ericson (YTF), Vincent McCovey (YTF), Larry Alameda (YTF), Steven Cantrell (CADFW), and Steve Strite (CADFW). Also, we would like to thank Jennie McSloy (BOR) for here help in editing this document.

LITERATURE CITED

Alvarez, J., D.H. Goodman, A. Martin, N.A. Som, K.A. Wright and T.B. Hardy. 2015. Development and validation of two-dimensional hydrodynamic models on the Trinity River, California. U.S. Fish and Wildlife Service. Arcata Fish and Wildlife Office, Arcata Fisheries Technical Report Number TR 2015-24, Arcata, California.

Buffington, J., C. Jordan, M. Merigliano, J. Peterson, and C. Stalnaker. 2014. Review of the Trinity River Restoration Program following Phase 1, with emphasis on the Program's channel rehabilitation strategy. Prepared by the Trinity River Restoration Program's Science Advisory Board for the Trinity River Restoration Program with assistance from Anchor QEA, LLC, Stillwater Sciences, BioAnalysts, Inc., and Hinrichsen Environmental Services.

Chamberlain, C.D., S. Quinn, B. Matilton. 2012. Distribution and Abundance of Chinook Salmon Redds in the Mainstem Trinity River 2002 to 2011. U.S. Fish and Wildlife Service. Arcata Fish and Wildlife Service Office, Arcata Fisheries Technical Report TR 2012-16, Arcata, California.

DeJuilio, K., A. Martin, J. Alvarez and D.H. Goodman. 2014. Age-0 Chinook and Coho salmon rearing habitat assessment: Sawmill rehabilitation site, three years after construction at winter base flow, upper Trinity River. U.S. Fish and Wildlife Service. Arcata Fish and Wildlife Office, Arcata Fisheries Data Series Report Number DS 2014- 37, Arcata, California.

Gelman, A. 2006. Prior distributions for variance parameters in hierarchical models. Bayesian Analysis. 1(3):515-533.

Gelman, A., J.B. Carlin, H.S. Stern, D.B. Dunson, A. Vehtari, and D.B. Rubin. Bayesian Data Analysis. Chapman and Hall/CRC Press. 2014

Goodman, D.H., A.M. Martin, J. Alvarez, A. Davis and J. Polos. 2010. Assessing Trinity River salmonid habitat at channel rehabilitation sites, 2007-2008. United States Fish and Wildlife Service, Arcata Fish and Wildlife Office, Tribal Fisheries Program, Hoopa Valley Tribal Fisheries Department. Arcata Fisheries Technical Report Number TR 2010-13, Arcata, California.

Graves, T.A., K.C. Kendall, J.A. Royle, J.B. Stetz, and A.C. Macleod. 2011. Linking landscape characteristics to local grizzly bear abundance using multiple detection methods in a hierarchical model. Animal Conservation 14(6):652-664.

Harris, N.J., Petros, P., and W.D. Pinnix. 2016. Juvenile Salmonid Monitoring on the Mainstem Trinity River, California, 2015. Yurok Tribal Fisheries Program, Hoopa Valley Tribal Fisheries Department, and U.S. Fish and Wildlife Service, Arcata Fish and Wildlife Office. Arcata Fisheries Data Series Report Number DS 2016-46, Arcata, California.

Hillman, T.W., J.W. Mullan, and J.S. Griffith. 1992. Accuracy of Underwater Counts of Juvenile Chinook Salmon, Coho Salmon, and Steelhead. North American Journal of Fisheries Management 12:598-603.

Kellner, K. 2014. jagsUI: run JAGS specifically, libjags) form R; an alternative user interface for rjags. https://github.com/kenkellner/jagsUI.

Kery, M. 2008. Estimating abundance from bird counts: binomial mixture models uncover complex covariate relationships. The Auk 125(2):336-345.

Kery, M., and M. Schaub. 2012. Bayesian Population Analysis Using Win BUGS. Academic Press. 554pp.

Kiefer, J. 1958. On the nonrandomized optimality and randomized nonoptimality of symmetrical designs. The Annals of Mathematical Statistics 29(3):675-699.

Miller, M.W., E.V. Pearlstine, R.M. Dorazio, and F.J. Mazzotti. 2011. Occupancy and abundance of wintering birds in a dynamic agricultural landscape. Journal of Wildlife Management 75(4):1937—2817. doi: 10.1002/jwmg.98.

Petros, P., N.J. Harris, and W.D. Pinnix. 2015. Juvenile Salmonid Monitoring on the Mainstem Trinity River, California, 2014. Hoopa Valley Tribal Fisheries Department, Yurok Tribal Fisheries Program, and U. S. Fish and Wildlife Service, Arcata Fish and Wildlife Office. Arcata Fisheries Data Series Report Number DS 2015-44, Arcata, California.

Pinnix, W.D., K. De Juilio, P. Petros, and N.A. Som. 2016. Feasibility of Snorkel Surveys for Determining Relative Abundance and Habitat Associations of Juvenile Chinook Salmon on the Mainstem Trinity River, California. Yurok Tribal Fisheries Program, Hoopa Valley Tribal Fisheries Department, and U. S. Fish and Wildlife Service, Arcata Fish and Wildlife Office. Arcata Fisheries Technical Series Report Number TR 2016-24, Arcata, California.

Plummer, M. 2014. JAGS: A program for analysis of Bayesian graphical models using Gibbs sampling. http://mcmc-jags.sourceforge.net/.

Polos, J. 2013. Scoping for the Development of a Salmonid Production Model for the Trinity River. Trinity River Restoration Program Salmonid Production Model Workshop. Arcata, CA 101 pp.

Royle, J.A. 2004. N-mixture models for estimating population size from spatially replicated counts. Biometrics 60:108-115.

Rupert, D. L., S. A. Gough, N. A. Som, N. J. Davids, W. C. Matilton, A. M. Hill, and J. L. Pabich. 2017. Mainstem Trinity River Chinook Salmon Spawning Survey, 2015 and 2016. U.S. Fish and Wildlife Service. Arcata Fish and Wildlife Office, Arcata Fisheries Data Series Report Number DS 2017–56, Arcata, California.

Som, N.A., R.W. Perry, E.C. Jones, K. De Juilio, P. Petros, W.D. Pinnix, and D.L. Rupert. 2017. N-mix for fish: estimating riverine salmonid habitat selection via N-mixture models. Canadian Journal of Fisheries and Aquatic Sciences 75(7):1048-1058. doi: 10.1139/cjfas-2017-0027.

TRRP (Trinity River Restoration Program) and ESSA (ESSA Technologies Ltd). 2009. Integrated Assessment Plan, Version 1.0 – September 2009. Draft report prepared for the Trinity River Restoration Program, Weaverville, California. 285 pp.

TRRP (Trinity River Restoration Program). 2014. Restoration Flow Releases on the Trinity River – Water Year 2013. Technical Report #TR-TRRP-2014-1. Trinity River Restoration Program, Weaverville, California.

TRRP (Trinity River Restoration Program). 2015. Restoration Flow Releases on the Trinity River – Water Year 2014. Work Group Report TR-TRRP-2015-1. Trinity River Restoration Program, Weaverville, California.

USBOR (U.S Bureau of Reclamation). 2009. Trinity River Restoration Program, channel rehabilitation and sediment management for remaining phase 1 and phase 2 sites—Part 1: draft master EIR and Part 2: Environmental Assessment/draft EIR. Trinity River Restoration Program, Weaverville, CA.

USDOI (U.S. Department of the Interior). 2000. Record of decision Trinity River mainstem fishery restoration, final environmental impact statement/environmental impact report.

USFWS (U.S. Fish and Wildlife Service). 1989. Annual report, Trinity River flow evaluation. U.S. Fish and Wildlife Service, Sacramento Field Office, Sacramento, California. 115 pp.

USFWS (U.S. Fish and Wildlife Service) and HVT (Hoopa Valley Tribe). 1999. Trinity River flow evaluation- final report. U.S. Fish and Wildlife Service, Arcata Fish and Wildlife Office, Arcata, CA and Hoopa Valley Tribe, Hoopa, CA. 308 pp.

APPENDICES

Appendix A. Dates of sampling rounds, flows during sampling (m^3s^{-1}), model run used (m^3s^{-1}), change in flows ($flow_{snorkel}–flow_{setup}$; m^3s^{-1}), and number of polygons created at the nine sample locations for 2013.

		Cableway	Bucktail	McIntyre	I.C. Boat Access	I.C. Side Channel	Evans Bar	Roundhouse	Sheridan	Valdor
Round 1 2/12 - 2/22	Flow at Gage	---	---	---	---	---	---	---	---	---
	2D Model Used	---	---	---	---	---	---	---	---	---
	Δflow (Dove - Map)	---	---	---	---	---	---	---	---	---
	Polygons Created	---	---	---	---	---	---	---	---	---
Round 2 2/26 - 3/7	Flow at Gage	8.55	8.55	8.69	11.75	8.95	14.69	14.05	---	18.37
	2D Model Used	8.5	8.5	12.7	15.6	15.6	19.8	19.8	---	24.1
	Δflow (Dove - Map)	-0.1	0.17	0	-1.4	0.23	-0.3	1.3	---	-0.2
	Polygons Created	59	40	40	40	48	25	51	---	28
Round 3 3/11 - 3/20	Flow at Gage	8.55	10.14	9.74	10.59	10.62	15.86	15.86	15.86	20.27
	2D Model Used	8.5	8.5	8.5	8.5	8.5	15.57	15.57	19.82	22
	Δflow (Dove - Map)	-0.28	-0.54	1.93	1.95	-0.23	0.17	0.17	1.05	0.48
	Polygons Created	57	47	46	38	54	47	46	41	46
Round 4 3/25 - 4/3	Flow at Gage	8.98	9.6	9.74	10.56	11.52	15.52	15.86	15.52	20.5
	2D Model Used	8.5	8.5	8.5	8.5	8.5	15.57	15.57	19.82	22
	Δflow (Dove - Map)	-0.28	-0.76	-0.2	-0.11	-1.25	0	-0.51	0.17	-0.23
	Polygons Created	58	40	56	35	50	41	45	45	45
Round 5 4/8 - 4/17	Flow at Gage	10.39	11.16	10.36	11.1	11.19	18.66	19.03	19.03	30.87
	2D Model Used	8.5	8.5	12.74	15.57	15.57	19.82	19.82	19.82	28.32
	Δflow (Dove - Map)	0.99	-1.25	-0.2	-0.2	-0.28	-0.17	-0.54	-0.54	-3.43
	Polygons Created	39	41	47	50	50	50	56	47	50
Round 6 4/24 - 4/30	Flow at Gage	55.5	55.9	---	---	60.88	---	---	59.75	63.43
	2D Model Used	56.63	56.63	---	---	56.63	---	---	56.63	56.63
	Δflow (Dove - Map)	-0.57	0.68	---	---	0.82	---	---	-0.57	2.27
	Polygons Created	57	44	---	---	43	---	---	41	42
Round 7 5/14 - 5/23	Flow at Gage	---	---	---	---	---	---	---	---	---
	2D Model Used	---	---	---	---	---	---	---	---	---
	Δflow (Dove - Map)	---	---	---	---	---	---	---	---	---
	Polygons Created	---	---	---	---	---	---	---	---	---
Round 8 5/28 - 6/6	Flow at Gage	---	---	---	---	---	---	---	---	---
	2D Model Used	---	---	---	---	---	---	---	---	---
	Δflow (Dove - Map)	---	---	---	---	---	---	---	---	---
	Polygons Created	---	---	---	---	---	---	---	---	---
Round 9 6/11 - 6/20	Flow at Gage	---	---	---	---	---	---	---	---	---
	2D Model Used	---	---	---	---	---	---	---	---	---
	Δflow (Dove - Map)	---	---	---	---	---	---	---	---	---
	Polygons Created	---	---	---	---	---	---	---	---	---
	Total Polygons per Site	270	212	189	163	245	163	198	174	211

Appendix B. Dates of sampling rounds, flows during sampling (m^3s^{-1}), model run used (m^3s^{-1}), change in flows (flowsnorkel–flowsetup; m^3s^{-1}), and number of polygons created at the nine sample locations for 2014.

		Cableway	Bucktail	McIntyre	I.C. Boat Access	I.C. Side Channel	Evans Bar	Roundhouse	Sheridan	Valdor
	Flow at Gage	8.55	9.03	9.32	9.63	9.83	12.18	15.69	11.27	15.12
Round 1	2D Model Used	8.5	8.5	8.5	12.74	12.74	12.74	15.57	12.74	15.57
2/10 - 2/20	Δflow (Dove - Map)	0	0.28	0.34	0	0	-0.91	-3.65	0	-1.53
	Polygons Created	40	27	48	36	35	33	38	39	24
	Flow at Gage	8.69	9.34	9.32	---	14.92	10.42	10.42	---	13.03
Round 2	2D Model Used	8.5	8.5	8.5	---	12.74	8.5	8.5	---	12.74
2/24 - 3/5	Δflow (Dove - Map)	0.14	-0.51	8.38	---	-1.19	0	0.14	---	-0.17
	Polygons Created	35	32	35	---	32	30	31	---	27
	Flow at Gage	8.98	11.86	12.15	12.88	11.3	16.2	12.94	12.94	19.26
Round 3	2D Model Used	8.5	8.5	8.5	12.74	12.74	15.57	15.57	15.57	19.82
3/11 - 3/19	Δflow (Dove - Map)	-0.71	0.48	-1.44	-1.59	-1.5	-2.76	-0.45	-0.62	-0.99
	Polygons Created	34	24	37	28	34	27	37	31	30
	Flow at Gage	8.27	9.09	9.15	9.2	9.2	11.27	11.72	18.49	---
Round 4	2D Model Used	8.5	8.5	8.5	8.5	8.5	12.74	8.5	15.57	---
3/24 - 4/3	Δflow (Dove - Map)	0.28	-0.54	-0.31	0.37	0.37	-0.28	0	0	---
	Polygons Created	39	36	36	38	31	30	40	30	---
	Flow at Gage	8.83	10.14	9.66	11.27	11.27	16.03	15.86	15.86	23.64
Round 5	2D Model Used	8.5	8.5	8.5	12.74	12.74	15.57	15.57	15.57	19.82
4/7 - 4/22	Δflow (Dove - Map)	-0.14	-0.65	0.17	-0.57	-0.57	-0.34	-2.75	-0.65	0.14
	Polygons Created	39	32	42	37	30	31	36	33	24
	Flow at Gage	---	---	---	---	---	---	---	---	---
Round 6	2D Model Used	---	---	---	---	---	---	---	---	---
4/28 - 5/8	Δflow (Dove - Map)	---	---	---	---	---	---	---	---	---
	Polygons Created	---	---	---	---	---	---	---	---	---
	Flow at Gage	41.06	41.68	42.76	42.36	43.52	43.89	43.32	43.04	45.02
Round 7	2D Model Used	42.48	42.48	42.48	42.48	42.48	42.48	42.48	42.48	42.48
5/13 - 5/22	Δflow (Dove - Map)	0.85	0.57	-0.23	0	-1.19	-0.28	0.57	0.85	-0.28
	Polygons Created	68	52	57	52	48	40	54	41	57
	Flow at Gage	32.56	32.71	33.41	34.09	33.81	29.45	29.45	28.88	29.45
Round 8	2D Model Used	33.98	33.98	33.98	33.98	33.98	28.32	28.32	28.32	24.07
6/3 - 6/12	Δflow (Dove - Map)	1.13	0.54	-0.57	-0.85	-0.59	-1.13	-0.57	-0.57	-3.09
	Polygons Created	58	49	26	52	43	40	50	48	50
	Flow at Gage	19.74	19.82	20	20.08	20.05	14.38	15.86	16.2	14.92
Round 9	2D Model Used	19.82	19.82	19.82	19.82	19.82	15.57	15.57	15.57	15.57
6/17 - 6/25	Δflow (Dove - Map)	-1.42	-1.44	-0.23	-0.03	-0.23	-0.17	-1.81	-2.15	0
	Polygons Created	59	51	53	51	49	41	51	53	44
	Total Polygons per Site	372	303	334	294	300	272	337	275	256

Appendix C. Example of data collected from one day of sampling at one site (Cableway).

Unique_ID	Year	Ordinal_Da	Date	Round	Site	Shape_Area	Off Channel?	Substrate in Polygon	Cover Type in Polygon	Cover Density Percentile	Nearest Cover Type	Distance to Cover	Bank edge?	Distance to Bank	Depth of Polygon	Velocity of Polygon	Depth Outside Polygon	Velocity Outside Polygon	diver_time	Diver 1 (Inside)	Water Visability	Chinook < 50mm D1	Chinook 50+mm D1	Coho < 50mm D1	Coho 50+mm D1	Steelhead < 50mm D1	Steelhead 50+mm D1	Brown Trout < 50mm D1	Brown Trout 50+mm D1	Diver 2 (outside)	Water Visability 2	Chinook < 50mm D2	Chinook 50+mm D2	Coho < 50mm D2	Coho 50+mm D2	Steelhead < 50mm D2	Steelhead 50+mm D2	Brown Trout < 50mm D2	Brown Trout 50+mm D2
CW1693	2014	49	2/18/2014	1	Cableway	18.53	No	Gravel	SWD	75-100%	NA	0	No	4	0.6	0.5	1.5	1.87	03:52:40pm	Thomas	5	0	0	0	0	0	0	0	0	Seth	5	0	0	0	0	0	0	0	0
CW1705	2014	49	2/18/2014	1	Cableway	106.13	No	Gravel	NA	0	SWD	79	No	12	0.6	0.15	2.1	1.39	04:07:39pm	Thomas	5	0	0	0	0	0	0	0	0	Seth	5	0	0	0	0	0	0	0	0
CW1700	2014	49	2/18/2014	1	Cableway	81.42	No	Gravel	NA	0	LWD	35	No	4	0.7	2.53	1.1	3.8	04:00:58pm	Andrew	5	0	0	0	0	0	0	0	0	Derek	5	0	0	0	0	0	0	0	0
CW1694	2014	49	2/18/2014	1	Cableway	46.36	No	Gravel	SWD	50-75%	NA	0	No	8	0.8	2.8	0.8	2.72	03:53:22pm	Thomas	5	0	0	0	0	0	0	0	0	Seth	5	0	0	0	0	0	0	0	0
CW1715	2014	49	2/18/2014	1	Cableway	58.95	Yes	Gravel	SWD	25-50%	NA	0	No	5	0.9	0.24	1.4	0.58	02:58:46pm	Andrew	5	41	0	0	0	0	0	0	0	Derek	5	51	0	0	0	0	0	0	0
CW1703	2014	49	2/18/2014	1	Cableway	91.79	No	Gravel	NA	0	LWD	89	No	7	1	0.6	2	2.35	04:12:27pm	Thomas	5	0	0	0	0	0	0	0	0	Seth	5	0	0	0	0	0	0	0	0
CW1713	2014	49	2/18/2014	1	Cableway	40.12	Yes	Gravel	LWD	<25%	NA	0	No	12	1	0.28	1.1	0.12	02:55:20pm	Andrew	5	0	0	0	0	0	0	0	0	Derek	5	1	0	0	0	0	0	0	0
CW1714	2014	49	2/18/2014	1	Cableway	55.08	Yes	Gravel	SWD	25-50%	NA	0	No	8	1	1	0.9	2.23	02:56:07pm	Andrew	5	0	0	0	0	0	0	0	0	Derek	5	0	0	0	0	0	0	0	0
CW1719	2014	49	2/18/2014	1	Cableway	33.78	Yes	Gravel	SWD	<25%	NA	0	No	5	1	0.37	1.4	1.08	03:10:33pm	Andrew	5	0	0	0	0	0	0	0	0	Derek	5	0	0	0	0	0	0	0	0
CW1712	2014	49	2/18/2014	1	Cableway	23.44	Yes	Gravel	NA	0	LWD	8	No	9	1.1	0.98	0.5	2.23	02:53:46pm	Andrew	5	0	0	0	0	0	0	0	0	Derek	5	0	0	0	0	0	0	0	0
CW1707	2014	49	2/18/2014	1	Cableway	21.72	Yes	Cobble	SWD	<25%	NA	0	No	8	1.2	1.71	1.2	1.7	02:43:38pm	Andrew	5	0	0	0	0	0	0	0	0	Derek	5	0	0	0	0	0	0	0	0
CW1720	2014	49	2/18/2014	1	Cableway	40.21	Yes	Gravel	SWD	50-75%	NA	0	No	5	1.2	0.76	1.6	1.14	03:11:13pm	Andrew	5	0	0	0	0	0	0	0	0	Derek	5	0	0	0	0	0	0	0	0
CW1721	2014	49	2/18/2014	1	Cableway	86.78	Yes	Gravel	SWD	<25%	NA	0	No	5	1.2	1.33	1.1	0.41	03:12:45pm	Andrew	5	0	0	0	0	0	0	0	0	Derek	5	0	0	0	0	0	0	0	0
CW1708	2014	49	2/18/2014	1	Cableway	19.53	Yes	Cobble	SWD	<25%	NA	0	No	12	1.3	0.62	1.3	1.75	02:44:53pm	Andrew	5	0	0	0	0	0	0	0	0	Derek	5	0	0	0	0	0	0	0	0
CW1710	2014	49	2/18/2014	1	Cableway	33.63	Yes	Cobble	LWD	50-75%	NA	0	No	17	1.3	0.73	1.4	1.04	02:47:02pm	Andrew	5	0	0	0	0	0	0	0	0	Derek	5	0	0	0	0	0	0	0	0
CW1711	2014	49	2/18/2014	1	Cableway	55.02	Yes	Gravel	SWD	75-100%	NA	0	No	13	1.3	0.35	1.4	1.77	02:51:22pm	Andrew	5	0	0	0	0	0	0	0	0	Derek	5	1	0	0	0	0	0	0	0
CW1697	2014	49	2/18/2014	1	Cableway	71.06	No	Gravel	UNDERCUT	<25%	NA	0	No	4	1.5	1.7	1.6	3.2	03:58:43pm	Thomas	5	4	0	0	0	0	0	0	0	Seth	5	4	0	0	0	0	0	0	0
CW1709	2014	49	2/18/2014	1	Cableway	52.32	Yes	Cobble	SWD	50-75%	NA	0	No	6	1.5	0.55	1.5	1.54	02:47:45pm	Andrew	5	14	0	0	0	0	0	0	0	Derek	5	19	0	0	0	0	0	0	0
CW1696	2014	49	2/18/2014	1	Cableway	161.08	No	Cobble	NA	0	SWD	44	No	11	1.6	1.8	2.3	1.7	03:54:06pm	Andrew	5	0	0	0	0	0	0	0	0	Derek	5	0	0	0	0	0	0	0	0
CW1698	2014	49	2/18/2014	1	Cableway	120.83	No	Gravel	NA	0	SWD	35	No	25	1.6	1.45	1.4	1.98	04:02:49pm	Thomas	5	0	0	0	0	0	0	0	0	Seth	5	0	0	0	0	0	0	0	0
CW1704	2014	49	2/18/2014	1	Cableway	62.98	No	Cobble	NA	0	SWD	6	No	10	1.6	0.03	1.8	0.74	04:08:55pm	Thomas	5	0	0	0	0	0	0	0	0	Seth	5	0	0	0	0	0	0	0	0
CW1706	2014	49	2/18/2014	1	Cableway	86.02	No	Gravel	NA	0	SWD	40	No	7	1.6	0.84	2.1	2.29	04:05:23pm	Thomas	5	0	0	0	0	0	0	0	0	Seth	5	0	0	0	0	0	0	0	0
CW1718	2014	49	2/18/2014	1	Cableway	80.90	Yes	Cobble	NA	0	BLACKBERRY	7	No	8	1.7	0.33	1.8	0.32	03:05:31pm	Andrew	5	0	0	0	0	0	0	0	0	Derek	5	0	0	0	0	0	0	0	0
CW1690	2014	49	2/18/2014	1	Cableway	36.34	No	Gravel	NA	0	LWD	50	No	15	1.9	1.11	2.1	1.1	03:46:17pm	Thomas	5	0	0	0	0	0	0	0	0	Seth	5	0	0	0	0	0	0	0	0
CW1699	2014	49	2/18/2014	1	Cableway	20.02	No	Gravel	NA	0	LWD	25	No	25	2	2.22	2.1	3.7	04:01:32pm	Andrew	5	0	0	0	0	0	0	0	0	Derek	5	0	0	0	0	0	0	0	0
CW1716	2014	49	2/18/2014	1	Cableway	50.63	Yes	Cobble	NA	0	SWD	10	No	17	2	0.61	2	0.57	03:02:28pm	Andrew	5	0	0	0	0	0	0	0	0	Derek	5	0	0	0	0	0	0	0	0
CW1717	2014	49	2/18/2014	1	Cableway	51.54	Yes	Gravel	NA	0	SWD	10	No	20	2	0.58	1.8	0.47	03:03:39pm	Andrew	5	0	0	0	0	0	0	0	0	Derek	5	0	0	0	0	0	0	0	0
CW1722	2014	49	2/18/2014	1	Cableway	42.70	Yes	Sand	NA	0	SWD	5	No	10	2	0.06	2	0.16	03:15:14pm	Andrew	5	0	0	0	0	0	0	0	0	Derek	5	0	0	0	0	0	0	0	0
CW1723	2014	49	2/18/2014	1	Cableway	31.27	Yes	Gravel	LWD	<25%	NA	0	No	4	2	0.59	2	0.67	03:16:17pm	Andrew	5	0	0	0	0	0	0	0	0	Derek	5	0	0	0	0	0	0	0	0
CW1695	2014	49	2/18/2014	1	Cableway	25.37	No	Cobble	NA	0	SWD	78	No	16	2.1	0.02	3	1.3	03:49:36pm	Andrew	5	0	0	0	0	0	0	0	0	Derek	5	0	0	0	0	0	0	0	0
CW1701	2014	49	2/18/2014	1	Cableway	49.55	No	Cobble	NA	0	SWD	100	No	18	2.3	0.87	2.5	1.05	04:03:44pm	Thomas	5	0	0	0	0	0	0	0	0	Seth	5	0	0	0	0	0	0	0	0
CW1702	2014	49	2/18/2014	1	Cableway	25.66	No	Gravel	NA	0	SWD	35	No	28	2.5	0.7	3.2	1.56	04:06:19pm	Andrew	5	0	0	0	0	0	0	0	0	Derek	5	0	0	0	0	0	0	0	0
CW1729	2014	49	2/18/2014	1	Cableway	23.82	Yes	Gravel	LWD	50-75%	NA	0	No	15	2.8	0.5	3.5	0.69	03:26:23pm	Andrew	5	0	0	0	0	0	0	0	0	Derek	5	0	0	0	0	0	0	0	0
CW1691	2014	49	2/18/2014	1	Cableway	24.12	No	Cobble	NA	0	LWD	40	No	35	3.1	1.96	3.5	1.3	03:45:16pm	Thomas	5	0	0	0	0	0	0	0	0	Seth	5	0	0	0	0	0	0	0	0
CW1692	2014	49	2/18/2014	1	Cableway	24.55	No	Boulder	NA	0	LWD	50	No	42	3.4	1.2	4	0.7	03:46:34pm	Thomas	5	0	0	0	0	0	0	0	0	Seth	5	0	0	0	0	0	0	0	0
CW1725	2014	49	2/18/2014	1	Cableway	18.55	Yes	Gravel	SWD	25-50%	NA	0	No	5	3.5	0.13	3.5	0.03	03:21:34pm	Andrew	5	0	0	0	0	0	0	0	0	Derek	5	0	0	0	0	0	0	0	0
CW1727	2014	49	2/18/2014	1	Cableway	27.39	Yes	Bedrock	SWD	<25%	NA	0	No	10	3.7	0.11	4	0.02	03:23:00pm	Andrew	5	0	0	0	0	0	0	0	0	Derek	5	0	0	0	0	0	0	0	0
CW1728	2014	49	2/18/2014	1	Cableway	63.66	Yes	Bedrock	NA	0	SWD	3	No	4	4	0.18	5	0.25	03:26:05pm	Andrew	5	0	0	0	0	0	0	0	0	Derek	5	0	0	0	0	0	0	0	0
CW1724	2014	49	2/18/2014	1	Cableway	40.92	Yes	Gravel	NA	0	LWD	3	No	17	4.5	0.06	4.5	0.18	03:20:19pm	Andrew	5	0	0	0	0	0	0	0	0	Derek	5	0	0	0	0	0	0	0	0
CW1726	2014	49	2/18/2014	1	Cableway	23.71	Yes	Gravel	NA	0	SWD	15	No	20	5.5	0.4	5.5	0.4	03:20:38pm	Andrew	5	0	0	0	0	0	0	0	0	Derek	5	0	0	0	0	0	0	0	0